

©2009

Mehdi Doumi

ALL RIGHTS RESERVED

A NEW, 3D OVERLAPPING-SPHERE MODEL OF CELL ADHESION

by

MEHDI DOUMI

A thesis submitted to the

Graduate School-New Brunswick

Rutgers The State University of New Jersey

and

The Graduate School of Biomedical Sciences

University of Medicine and Dentistry of New Jersey

In partial fulfillment of the requirements

For the degree of

Master of Science

Graduate Program in Biomedical Engineering

Written under the direction of

Dr. Troy Shinbrot

And approved by

New Brunswick, New Jersey

October, 2009

ABSTRACT OF THE THESIS

A New, 3D Overlapping-sphere Model of Cell Adhesion

by MEHDI DOUMI

Thesis Advisor: Dr. Troy Shinbrot

Cell adhesion refers to the ability of cells to make enduring and dynamic attachments to extracellular surfaces and to each other; rightly so it is a focal point of current biological research. I have designed a computational framework to model cell adhesion using a modified overlapping-sphere model. A core feature of the model is the three-dimensional representation of a cell surface that can interact mechanically with its environment. The generalization of a cell as a sphere gives our model the compactness to enable the simulations of thousands of cells, comparable to the number of cells typically encountered through small scale studies of early development and disease. Specifically, we use this computational framework to model adhesion between cells in a monolayer and a fibrous environment, cell shape change, as well as cell replication. We also include elements of cell orientation, or cell polarity, and touch on some aspects of mechanical feedback. We explore some general aspects of developmental biology as well as cancer in mammary ducts. Although we emphasize epithelial cells, which are cells that form monolayers, we also briefly consider migratory cells. The major results are that (1) Cells in a monolayer, like sheets and tubes, need to be both mobile and well-connected to adapt to mechanically stresses, (2) Cells that are not polarized do not produce a stable monolayer of cells, (3) Extracellular support, like a basement membrane, can minimize the stresses experienced at cell-cell junctions, (4) Mitosis triggered by tension can help maintain a monolayer of cells,

(5) Cell shape needs to be incorporated into models to minimize undesirable stresses, (6)

Our computational framework is useful to predict behavior of cells subjected to mechanical forces. As this is a new model, results are chiefly qualitative, and suggest future work in collaboration with experimentalists to verify and quantitate our results.

ACKNOWLEDGEMENTS

Advisor Dr. Troy Shinbrot for his course in mathematical modeling of self-assembly; funding my research for the last two years; supporting a 3-month research trip to ETH, Switzerland; teaching me the idea that complex events can be a result of simple rules; and for countless discussions in and out of the lab regarding science and academia.

Committee member Dr. David Shreiber for his course in biomechanics; letting me present my work at his lab meeting; and for several conversations on research.

Committee member Dr. Stanislav Shvartsman from Princeton University for letting me present my work to his lab; advising on specific research topics; and having an open door policy.

Committee member Dr. William Craelius for encouraging my research.

Lab members Carlos Caicedo, Kerri-Ann Norton, and Andrew Voyiadjis for their questions during lab meetings and passionate chats over coffee.

My family and friends for supporting everything else.

TABLE OF CONTENTS

ABSTRACT OF THE THESIS	ii
ACKNOWLEDGEMENTS	iv
TABLE OF CONTENTS.....	v
LIST OF FIGURES	vii
INTRODUCTION	1
Challenges of cell research	2
Cell Adhesion and Cell Mechanics	4
Adhesive potential	6
Polarity	7
Measuring mechanical properties	7
Computer Modeling of Cell Adhesion.....	10
MODEL	15
Model background	15
Physical description of model.....	17
Multiple Adhesion Molecules and Adhesive potential	22
In Aggregates, Initial Adhesion Formation is Based on Distance Thresholds	22
In Monolayers, Initial Adhesion Formation is Based on Orientation Information Too	23
Two Models for a Basement Membrane.....	24
Assumption on adhesion formation.....	25
Dynamics of cell adhesion	26
Modeling the Proliferation of Cells	27
Modeling Cell Shape and Morphogenesis	28
Computational Considerations.....	30
RESULTS AND DISCUSSION	33
Adhesion formation, adhesive potential and differential adhesion	33
Planar Cell Monolayers	38
Slipping vs. Non-slipping Interfaces between Cells in Monolayers.....	41
Cell Proliferation.....	45
Cell Tubes and the Importance of Polarity.....	47
Cell Shape and Morphogenesis.....	50
Three-dimensional tissue-deformation	52
Patterning of Cells Monolayers for Deformation.....	53
Exploring Cell-Substrate Interactions	56
CONCLUSION.....	60
Advantages to cytoskeleton vectors	61
Feedback to Growth	62
Membrane is domain for activity	62
NEXT STEPS.....	64
Polarity development	64
Contact Area	66
A Flexible Biological Model.....	68

APPENDIX.....	70
Derivation of viscous force.....	74
Algorithm Pseudo code.....	77
BIBLIOGRAPHY	79

LIST OF FIGURES

Figure 1. Schematic of cell adhesion components.	5
Figure 2. Variety of mechanical models to simulate biology. (a) Mechanical models require atleast one energy-storing element (green color) that releases energy in the form of a force over a distance. The force is parametrized by some elastic modulus or a spring stiffness coefficient. (b) In biological cells, the source of mechanical energy is distributed throughout the cell, though research has identified the adhesive bonds between adhesion molecules and the cytoskeleton as the prominent sources.	13
Figure 3. Comparing overlapping-sphere model with new model. (a) Attraction and repulsion forces are acted on the centers of the cells. (b) In new model, attraction forces are acting on the surface of the cell which can induce a torque, while repulsion forces act on the center of the cell.	16
Figure 4. (a) Overlapping with another cell causes a repulsive force to push against both cells in proportion to the overlap distance, d_{overlap} . (Only the one overlapping force vector is shown.).	18
Figure 5. (a) A cell experiencing a force due to cell-cell or cell-substrate adhesion, F_{adh} , at point $(x+r_1)$ also experiences a moment as a result of the adhesion. (b) The net force and moment translate and rotate the cell, respectively.	19
Figure 6. A pair of cells adhered to each other push and pull each other when the adhesive link is located far from the line connecting their cell centers. (b) Adhesive force is zero to ensure that compressive resistance forces are controlled by the koverlap parameter only.	20
Figure 7. (a) Multiple adhesion forces, F_{adh} , act simultaneously with compressive forces, F_{overlap} . (b) A view of a sheet of cells from actual simulation shows cell spheres overlapping and connected to each other's spherical surface by adhesive links (green lines).	21
Figure 8. Like a standard overlapping-sphere model, modeling cell aggregates in 3D, we use a distance threshold before forming an adhesion. This distance, d_{pseudo} , is proportionate to the actual length of the average pseudopodia that cells actually extend during early development when probing their environment. For cells in monolayers, however, this is done differently.	23
Figure 9. Specifying locations on the cell surface for a new adhesive link is possible using a point on the surface as a reference like vector, p . (a) The angular distance between regions on the surface of a sphere using the cytoskeleton vector, r_i , and polarity vector, p , is simply the inverse cosine of the vectors' dot product. (b) I evaluated a polarity model whereby spheres may only bind to each other at a specific.	23
Figure 10. Mitosis is modeled by replacing the mitosing sphere by two overlapping spheres connected by an adhesive link of natural length, L_0 . Over time L_0 is reduced to 0, the default length for a cell-cell adhesive link. This ensures that new cells gradually grow into place instead of causing a new cells to suddenly be ejected out of a monolayer due to the large repulsive forces caused by overlap with new neighbors.	27
Figure 11. Cell shape change can cause tissue deformation. (a) Cells adhered to each other via a mechanical spring. (b) Reorienting a cytoskeleton vector (black arrows) of center cell relative to the cell's polarity (dotted arrow) changes spatial location of an adhesive interface, thus reshaping the cell. (c) Cells are rotated and displaces until adhesive link attachment points are touching and the cytoskeletal vectors are aligned.	29
Figure 12. (a) A meshed sphere is the basic cell for a typical ADS model (Hammer and Apte 1992). It would be impractical to assume adhesion receptors exist at these mesh points and form adhesion between adjacent mesh points. Calculation time of such distances (b, drawn as colored lines) would grow exponentially (c) with the number of cells and mesh-points per cell.	31
Figure 13. Cell-cell adhesion formation. (a) Sixteen cells with equal adhesive potential arranged in a regular Cartesian grid. Color of cell is proportional to adhesive potential: hot-colored cell indicates cell is capable of binding to more cells than cold colored cell. (b) Adhesion contact between adjacent cells represented by the <i>adhesive link</i> (green lines). Note the change in adhesive potential once a cell binds to a neighbor.	33
Figure 14. Cells of different adhesive potential. Sixteen cells in the xy-plane are allowed to make a	

maximum number of adhesive links, from 0 (dark blue) to 4 (dark red). The white arrows show the direction of the net force vector acting on each cell.....	34
Figure 15. Adhesive potential on cell aggregates. Cells randomly clustered in space are each capable of making (a) 4, (b) 16, and (c) 64 adhesive links (green lines), effectively increasing their adhesive potential. Over time the cells (c) with the higher adhesive potential pack tighter. In this example, cells are capable of making multiple adhesive links with each of their neighbors.	35
Figure 16. Red cells can make double the number of links as green cells over time this disparity in adhesive potential causes the green cells to envelope the red cells.	36
Figure 17. The perturbation of a sheet of cells for two different area moments, (a) $I_0=1$ and (b) $I_0=10$. This parameter effectively changes the rotational rigidity of the cells, or how well connected the internal cytoskeleton is. Hot colored cell experience tension while cooler colors experience compression.	39
Figure 18. Basement membrane model. (a) Force perturbs a monolayer of cells, immovable at the edges (grey cells). (b) The same force perturbs a monolayer with a basement membrane and a different stress pattern appears. Hot colored cell experience tension while cooler colors experience compression.....	39
Figure 19. A hexagonally packed sheet of 64 cells existing freely in space is perturbed by a force (pink arrow), $F = 5$ in the z-direction on a corner cell. (a) Adhesive link by default are fixed to the surface of the sphere model surface and transmit torques through the cell causing an almost continuous bend through the group cells. (b) Allowing the adhesive links to slip along the surface caused sliding of layers of cells. Hotter colored cells experience tension; cold cells experience compression.....	41
Figure 20. A hexagonally packed sheet of 256 cells existing freely in space is perturbed by a force (pink arrow), $F = 5$ in the z-direction on the centermost cell. (a) Adhesive links by default are fixed to the surface of the sphere model surface and transmit torques through the cell causing almost continuous sheet-like undulations through the group of cells. (b) Adhesive link slipping permits sliding of cells and breaking of adhesive links. Hotter colored cells	43
Figure 21. Mitosis in a sheet of cells. Computationally, cells separate by a spring, connecting opposite surfaces of two overlapping spheres, that reduces its natural length to zero. Colored by youth, hotter cells are younger than colder cells. (Top view)	45
Figure 22. Feedback between tension and mitosis (top view). Cells demarcated by the white box are perturbed with a constant force to the right, while we employ a rule that states only cells under tension are allowed to mitose.....	46
Figure 23. The demand for polarity is high especially in complex geometry. (a) Cylindrical arrangement of unpolarized cells can bond to any membrane surface and proliferation quickly causes the hollow structure to disappear. (b) Restricting cell-cell attraction to a band (dotted green line) around each cell (red sphere) to simulate a lateral adhesion in epithelia, as well as a mechanical spring (blue line) to simulate basement membrane stiffness between the basal poles of cells, we approach a more accurate picture of epithelial tubes.	47
Figure 24. White arrows point to the cleavage plane of mitosing cells.....	48
Figure 25. (a) Changing the cytoskeleton vectors (black arrows) relative to a known direction defined by polarity vector, p . The adhesive link (green lines) provides the pulling force causing the overall tissue deformation see in (b) simulation (where cytoskeleton vectors are red lines).....	50
Figure 26. The effect of adhesive attraction during invagination. Six cells (red spheres) out of 32 cells become change from a cuboidal shape to a wedge-shape. The wedge acuteness is controlled by parameter $\Delta\theta$ which is the difference in angle between the current and final cytoskeletal vector directions. The boxed image is when $k_{adh} = k_{overlap} = 1$. Clearly a strong adhesion promotes invagination event.	51
Figure 27. The effect of compressive resistance during invagination. The boxed image is when $k_{adh} = k_{overlap} = 1$. A stiffer cell appears to transmit the forces due to shape change better than a soft cell, promoting invagination.....	51
Figure 28. Compressive stiffness parameter, $k_{overlap}$, effect on an invaginating tube. During development, global structure change is accompanied by the changing of shape of a small set of cells. In comparing invagination depths, we find proper transmission of forces due this shape change requires cells to be sufficiently rigid.....	52
Figure 29. Adhesive link stiffness parameter, k_{adh} , effect on an invaginating tube.....	53

Figure 30. Patterning a sheet of cells is crucial to formation of the right kind of structure.....	54
Figure 31. Migration on a stiffness gradient driven by cell-substrate adhesion. Substrate becomes stiffer as background color become hotter. Adhesive links (red lines) connect sphere surface (red spheres) to a random location in space (end of red line). Each point in space provides a spring coefficient for the adhesive link to simulate the amount of force that can be produced by the contractile machinery of that cell. Adhesive links on one side of the sphere compete with those on the opposite side.....	56
Figure 32. Thirty simulations reveal migratory trajectories are dependent on the number of adhesive links per cell (left column) and the relative steepness of the substrate stiffness gradient (bottom row). Cells on average move towards the stiffer side (right side) of substrate but through a variety of trajectories. Overlaid text shows the mean tortuosity of the trajectories and the variance of the tortuosity of the trajectories.....	58
Figure 33. Standard overlapping sphere model modified with polarity formation. Cell centers (black dots) attract each other according to distance-thresholds while the orientation of each cell-cell interface (red lines) contributes to the orientation of each cell's polarity axis (black lines).	65
Figure 34. (a) Using vectors to represents the centers of a contact area, one can compare the direction and location of. (b) We may even be able to make distinctions between cell-cell contacts and cell-substrate contacts based on the size of the contact area and their frequency of formation.	66

INTRODUCTION

Cell adhesion refers to the ability of cells to make enduring and dynamic attachments to surfaces and to each other, and rightly so it has been a focal point of current biological research. Cell adhesion has major implications in development and disease, and is also a regulator of cell identity, growth, movement, immune responses, and communication. The effects of adhesion are complex, and consequently models have been devised to test current research perceptions and predict cellular behavior *in silico* that would be otherwise too difficult to test *in vitro* and *in vivo*. In this thesis, I present a computational framework to model cell behavior due to cell adhesion. Specifically, I have modified previous work from Dr. Troy Shinbrot that focused on cell rearrangement in 3D aggregates, folding of a 2D monolayer (Shinbrot 2006) and pattern formation in 2D mammary ducts (Shinbrot and Norton 2009), to allow for a more detailed representation of cell adhesion. The computational framework is applied to epithelial cell tissues, which are cells organized in monolayers (one-cell thick sheets). Briefly, I have also tested this model to consider motility of mesenchymal cells. Both cell types play a role in early tissue development, which shares features with cancer development. The goal therefore is to assess what kind of physical structures are possible given a limited set of adhesion parameters within the context of development and cancer. In doing so, I also evaluate the model with respect to current models, to answer whether this innovative computer framework is relevant to modern biological research.

Challenges of cell research

The word “cell” initially described one of the many hexagonal spaces that make up cork, but eventually it became known as the fundamental unit of life responsible for self-replication and structural integrity in multicellular organisms (Mazzarello 1999; Karp 2008). We now realize that cells are capable of more complicated tasks: regulation of events like mitosis and death, differentiation into specialized cell types, and networked communication with other cells in an organism. It can only be admired that a single, fertilized egg cell can develop into a 10-trillion-cell human body.

Modern biological research has taken multicellular life and placed it in a glass dish, in order to understand the mechanisms behind development and disease at the cellular scale. In 1951, for example, the biologists at Johns-Hopkins University were the first to grow and maintain human cells in a Petri dish (Karp 2008).

Through research over the intervening several decades, it has become possible to measure chemical and physical properties of cells. One property that is the focus of this thesis are the biomechanical stress-strain relations of the cell and the resulting properties of the population of cells, be they in an aggregate or in a monolayer. It is important to discuss cells from the mechanical point of view, as many have (Odell, Oster et al. 1981; Dirk Drasdo 2000; Murray 2001), because the physical structure is visually measurable and latest technologies have made it possible to calculate exactly what stresses are present at micron-scale regions in biological tissue (Martin, Kaschube et al. 2009). To put the present work into context, we remark that the busy chemical environment within and without the cell has led to a common conviction that developmental and pathological mechanisms are purely genetic in nature, and that they are caused by a complex orchestra of chemical signals. This thesis’ point of view quietly positions itself with no assumption of genetic determination, to

ask whether it is possible – just by mechanical forces induced by cell adhesion and other physical constraints – to develop the sort of intricate geometries that occur during development of a gastrula, maintenance of tubular gland, and formation of cancer in the breast.

The importance of such a study is clear when one considers the recent failures in adapting tissue engineering technologies into real-world products, such as artificial organ implants and custom-designed cells (Griffith and Swartz 2006). Between 1995 and 2003, billions of dollars were effectively lost when companies engaged in cell-based tissue engineering failed to transition results from the research phase into a viable product phase (Lysaght and Hazlehurst 2004). Skin-cell (epidermal) engineering, for example, failed to provide skin-healing solutions for millions of burn victims and cosmetic procedures worldwide (Kim 2008). It is clear that a more thorough picture of cells must be painted before we can expect these crucial technologies to realize themselves in hospital procedures.

While *in vivo* experiments remain difficult to develop, and *in vitro* models struggle to narrow the range of behaviors cells display (Griffith and Swartz 2006; Kim 2008) especially as *in vitro* conditions are artificial and the cells used are immortalized. *In silico* models can provide insight into the range of outcomes that can be expected during *in vivo* and *in vitro* experiments. When the number of variables is high, as they are in cell research, a basic model can be supportive, both to provide comparisons between heuristic expectations and rigorous first-principles analysis and to suggest and evaluate new hypotheses.

Cell Adhesion and Cell Mechanics

Cells adhere to a surface when special molecules (adhesion molecules) entrenched within the cell membrane bind to complementary molecules in the cell's environment. For a cell-cell adhesion, the complementary molecule is usually the same adhesion molecule (homophilic binding). The cadherin family of molecules are proteins that bind to each other and connect cell surfaces in a zipper-like fashion – each new cadherin-cadherin bond promotes another nearby. For a cell-substrate or cell-matrix adhesion, the complementary molecule sits in the extracellular space as part of an extracellular protein matrix. Because the action of adhesion can be interpreted as one molecule “receiving” another molecule to bind to, adhesion molecules are often called receptors, thus translating cell-cell adhesion to receptor-receptor binding, and cell-substrate to receptor-ligand binding (Lauffenburger and Linderman 1993). This has added meaning when one considers the fact that as an adhesive interface matures it plays a larger role in receiving and transmitting mechanical and chemical signals.

From a macroscopic view, cell adhesion to a surface has the appearance of the cell spreading over the surface. An adhesion forms bond by bond, receptors attach to extracellular ligands or receptors. Cell peeling is the reverse of cell spreading, and occurs when receptors break their bonds with their adhesive surface (Lauffenburger and Linderman 1993). Recently, researchers have identified a type of adhesion bond called a “catch bond” that fosters new molecules to bind when it experiences mechanical stress (Thomas 2008). (Conversely, “slip bonds” weaken under stress.) In the case of catch bonds therefore, two cells would strengthen their attachment to one another upon experiencing stress. This is one example of a counter-intuitive phenomenon that gives merit to the idea of mechanical-based signals. Adhesion formation can also be modulated by the amount of lateral attraction between like adhesion molecules (Yeagle 2005; Karp 2008), as well as

lipid-protein interactions as is the case with between E-cadherin and Phosphatidylinositol-4,5-diphosphate (PIP2) (Sheetz, Sable et al. 2006).

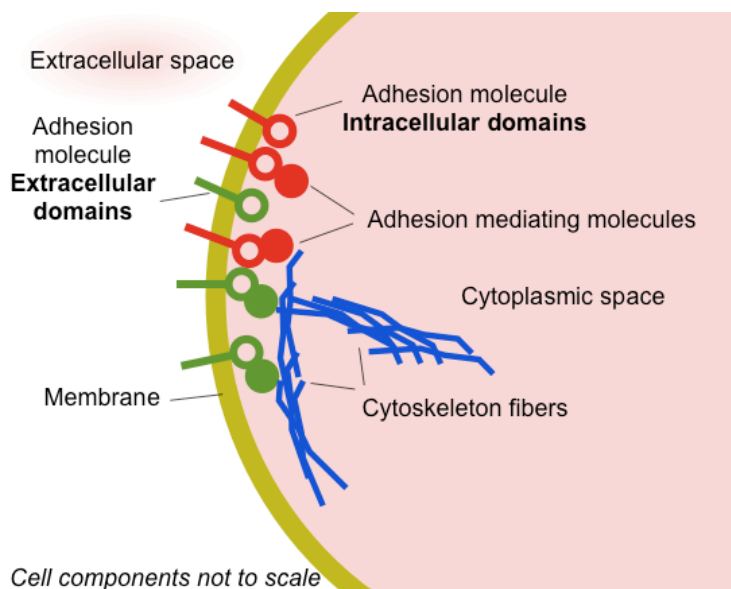


Figure 1. Schematic of cell adhesion components.

Cross-membrane adhesion molecules are attached to the cytoskeleton within the cell, which gives cells the ability to (1) resist compression, (2) resist tension, and (3) actively contract. The cytoskeleton is the scaffolding that mechanically supports a cell. As an adhesive contact matures, the adhesion molecules form bonds internally with the cytoskeleton, essentially creating a mechanical link between the intracellular cytoskeleton and the extracellular environment. Naturally, different cell types possess different mechanical properties due to their cytoskeleton makeup. A dilute solution of intermediate filaments (IF), one of the three known type of cytoskeleton fiber, has a shear modulus on the order of 1 Pascal (Pa, or Newton per square meter); whereas a 1000-times higher concentration in the cytoplasm of skin cells (epidermis), has an elastic modulus in the MPa range (1 million Pa). Increased cross linking of the IFs can further boost the elastic modulus to the GPa range (1 billion Pa) as in the case of nail and hair cells (Herrmann, Bar et al. 2007).

A cell can also contract parts of its cytoskeleton during migration, or the entire cytoskeleton when it is part of muscle tissue. Myosin proteins act as motors that pull actin protein filaments together to produce intracellular tension (Lecuit and Lenne 2007); healthy functioning of these actin-myosin motors is essential for breathing, circulating blood, peristalsis and locomotion (Herrmann, Bar et al. 2007). Tension is also produced laterally *across* the surface of cell-cell interfaces in order to maintain a rigid multicellular entity (Lecuit and Lenne 2007). This type of tension is called cortical tension because it exists at the periphery of the cytoplasm, or cell cortex. It is at this cortex that the cytoskeleton is able to transmit forces to and from the extracellular environment because the intracellular domains of adhesion molecules connect to cytoskeleton fibers. Cortical tension therefore plays an important role in the mechanics of cell-cell contacts.

Adhesive potential

The adhesive potential of a cell refers to the probability that a cell will form an adhesive and is often connected to the so-called Differential Adhesion Hypothesis (DAH) (Steinberg and Poole 1981). DAH asserts that cell populations can organize themselves simply due to differences in their adhesive potential, as long as they have freedom to rearrange themselves fluidly. Testing hypotheses like this is possible thanks to modern imaging technology, such as fluorescent-imaging techniques (Yeaglel 2005), and advances in genomics which give biologists control over what adhesion molecule-encoding genes are turned on and off (Tepass, Truong et al. 2000; Steinberg 2007). Defining adhesion molecule movement at submicron scales however has proven to be difficult since the membrane is not perfectly fluid (Pollack 2001,); there are numerous interactions between adhesion molecules and other, membrane- and cytoplasm-bound molecules (Yeaglel 2005); the membrane is littered with immobile “posts” (Zhang, Crise et al. 1991); and adhesion molecule membrane concentration is also a function of cytoplasmic concentration (Hammond, Sim et al. 2009). Data on the spatial properties of adhesion molecules lack

precision and consistency among research labs, which is probably why there have been many theoretical attempts over the years to estimate adhesion molecule parameters (Bell 1978; Lauffenburger and Linderman 1993; Ward, Dembo et al. 1994; Altschuler, Angenent et al. 2008; Liu, Montana et al. 2008; Thomas, Vogel et al. 2008). In summary, we can only make rough measurements of the number or concentration of adhesive bonds that are present at the cell surface.

Polarity

It is feasible to fluorescently-observe different adhesion molecules on the surface of a cell, as is commonly done *in vitro* to observe the general distribution of adhesion molecules (Citi 1993; Yamada and Clark 2002). These and other studies have proven that cells have a polarity (Drubin 2000), which refers to the internal rearrangement of organelles that specializes the surface of a cell so that it interacts with its environment in a directional fashion. Epithelial cells have integrin-type, cell-substrate, adhesion molecules that bind to extracellular matrix on their basal side. The lateral sides of these cells support cadherin-type, cell-cell adhesion molecules, that bind to adjoining cells. While the mechanisms underlying the formation of cell polarity remain to be fully elucidated, it is accepted that differences in cell type, cell function, and cell structure are related to the species and distribution of adhesion molecules. As a result the computational framework that we will describe shortly includes multiple types of adhesion.

Measuring mechanical properties

Finally, *in vitro* methods to measure the mechanical properties of cells are growing in number to provide a diverse set of measurements to which *in silico* methods can be compared. The first force measurements can be traced to Dale Rex Coman who used precalibrated microneedles to pull apart pairs of cells (Coman 1944). To study how

populations of cells rearrange, say to test the Differential Adhesion Hypothesis, a hanging-drop experiment gives cells unlimited freedom to move among themselves in a fluid environment; a loading test on the ball of cells later provides quantitative measurement of the cohesion of the aggregate (Foty and Steinberg 2005). Cells restricted to monolayers *in vivo*, like skin cells, are studied in the lab by placing cells on an artificial platform that mimics a basement membrane, to encourage lateral cohesion (Colgan 2006). More advanced techniques use layering of gel sheets containing cells, in order to simulate a native, three-dimensional *in vivo* environment. Each sheet can be “painted” (pre-patterned) with molecules, in any pattern, to stimulate cell traction and other cellular responses (Griffith and Swartz 2006).

In the study of cell movement, cellular traction forces can also be inferred through the stress lines of deformable rubber sheets (Harris, Wild et al. 1980; Karp 2008). Traction forces can additionally be derived through the displacement of fluorescent microbeads in gels of known elastic moduli (Roy, Rajfur et al. 2002). Cells moving on surfaces studded with nanometer-scale posts cause deflections of these posts, so the post-surface-density and extent of post-deflection can provide data on the force applied by the cell (Hallstrom, Martensson et al. 2007).

Unfortunately, different *in vitro* methods give differing measures of mechanical properties of cells, which is why there is little consensus among researchers as to what is, for example, the stiffness modulus of a cell. For the sake of this *in silico* study therefore, the biological parameters used are restricted to unitless values.

To summarize the key facts described above and elsewhere:

- (1) Gene expression level of cadherins can affect the adhesive potential of a cell, so some cells may be more “adhesive” than others, thus changing the interfacial

dynamics of a population of cells.

- (2) Adhesion formation is a function of the adhesion molecules, cell membrane environment, whether the molecules are catch or slip bonds, and internal cytoskeleton rearrangements due to polarity.
- (3) Adhesive plaques form when internal cytoskeleton binds to the adhesion molecule to form a mechanical linkage between the extracellular and intracellular environment (Drubin 2000).
- (4) A cell has a cytoskeleton that provides compressive resistance, tensile resistance and contractile forces.
- (5) Cortical tension at cell-cell interfaces can produce rigid cells.
- (6) Resistance to pulling a cell requires an adhesive interface and cytoskeleton support, so conceptually separating one from the other is difficult task.
- (7) The mechanism underlying the formation of cell polarity is still not fully understood but the resulting heterogeneous distribution of adhesion molecules is a known fact.
- (8) This computational framework considers unitless values for cell properties.

Computer Modeling of Cell Adhesion

Computer simulations can provide a quick, graphical, and realistic analog of biological processes (Bell 1978; Murray 2001; Davies 2005). There is a variety of computer models that approximate biology and typically a specific methodology is more appropriate for certain cell types over others. In the subsections following, we overview several leading methods that have been used to model cells and cell adhesion, and we relate these to our model.

FEM

Epithelial and endothelial tissues have most often been represented by finite-element methods, which solve constitutive equations in order to calculate the deformation of a polygonal figure made up of individual lines (in 2D) or polygons (in 3D). Finite element models (FEMs) have been typically constrained to two dimensions (Brodland and Veldhuis 2002; Brodland, Chen et al. 2006) as three-dimensional simulations are more computationally intensive and require careful schemes to accurately correct for changes in cell volume (Conte, Munoz et al. 2008).

One assumption that FEM models commonly make is that biology structures, like a gastrula, are symmetric so half of the geometry is calculated and then mirrored. This makes it impossible to test whether epithelial tissue deformation is induced by random perturbations of a couple of individual cells. There is evidence, after all, that during tissue deformation during *Drosophila* development, cells contract erratically (Martin, Kaschube et al. 2009).

Additionally, with a rectangular mesh a finite-element model does not model individual cells, it models a continuum discretized into regular, usually cuboidal, polygons. Even still,

these polygons do not necessarily represent a cell. Events like cell rearrangements in-plane (Citi 1993) are therefore impossible to capture.

Spring network models

Though not technically a FEM, the 2D purse-string model (Odell, Oster et al. 1981) simulates cells in a cross-section of a hollow blastula. The vertices of contact between its quadrilateral cells are connected by damped springs, effectively making each of the four edges of each cell, elastic. Using a set of springs instead of a continuous media to model elasticity it is possible to simulate tension at specific regions of cells – for example, the apical surface - which is suspected to cause the fundamental tissue deformations during development.

The advantage of this purse-string model lies in its simplicity; the spring elements are attributed to biological cytoskeleton elements. Our computational model also use a spring element to correspond to the cytoskeleton. Like an FEM however, the purse-string model does not allow cells to change their neighbors. Finally, the purse-string model has remained a two-dimensional model.

Single-cell models

For motile cells, FEM or spring networks are not useful because in such models, cells are fixed in place and can deform, but typically cannot detach or relocate. Therefore, the movement of cells through space in single-cell models, individual cells are modeled as objects, or agents, in space that can attract or repel each other to mimic cell adhesion. The Adhesive Dynamics Simulation (ADS), pioneered in 1992 by Hammer and coworkers (Hammer and Apte 1992) models a leukocyte cell as a viscoelastic sphere layered with a microvilli, which is then covered with receptors that make spring-like connections with a substrate. ADS has since evolved to model multiple leukocytes, viscoelastic microvilli, fluid flow in a bloodstream, stochastic receptor binding rules, and multiple receptor types

(Gillespie and Walker 2001; King and Hammer 2001; Bhatia, King et al. 2003; Pappu, Doddi et al. 2008). In this approach, cell-substrate attachment is controlled by parameters defining molecular binding kinetics, and under fluid flow, the cell deforms. The success of ADS is directly related to the fact that it models a highly localized system at small time scales (~seconds), making it reproducible both *in vivo* and *in vitro* (U H von Andrian 1993).

Modeling thousands of cells as in an epithelial sheet in equivalent detail is computationally intensive. Rejniak therefore simplifies cells as fluid-sacks in two-dimensions and incorporates the breaking and forming of springs to adhere cells together in a dynamic fashion (Rejniak 2005). Three-dimensional overlapping-sphere models use attraction based on distances from sphere centers. Extending this idea to ellipsoids, Palsson designed an overlapping-ellipsoid model that includes attraction through the attachment of springs to connect ellipsoidal surfaces cells (Palsson 2008). Unlike the models of Hammer and Rejniak, where the springs represent adhesion molecules binding, overlapping-sphere models use springs to represent a larger feature of biology: the cytoskeletal elements that span the cytoplasm and connect to intracellular portions of the adhesion molecules. This way, fewer spring forces need to be parameterized, measured and integrated, than if each spring were to represent an individual adhesion molecule.

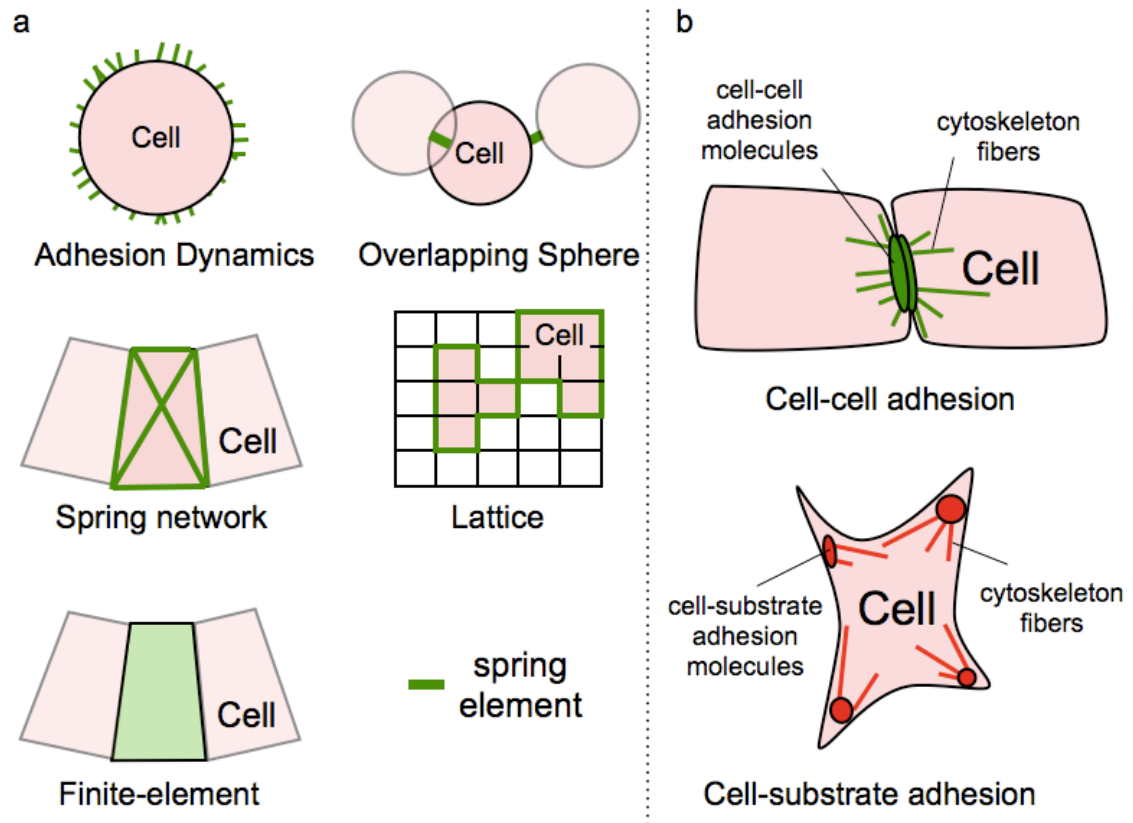


Figure 2. Variety of mechanical models to simulate biology. (a) Mechanical models require at least one energy-storing element (green color) that releases energy in the form of a force over a distance. The force is parametrized by some elastic modulus or a spring stiffness coefficient. (b) In biological cells, the source of mechanical energy is distributed throughout the cell, though research has identified the adhesive bonds between adhesion molecules and the cytoskeleton as the prominent sources.

To summarize:

- (1) 3D Finite element models are optimized for modeling continuous volumes like cell monolayers but are not detailed enough to consider individual cells and interfaces. 2D finite-element models are more successful in this regard.
- (2) Spring network models (Odell, Oster et al. 1981) have not been extended to 3D, but they are detailed enough to make connections between the global cell monolayer structure and the intercellular properties.
- (3) Single-cell models provide the most detail per cell, including local rearrangement of cell neighbors, however they are never used to simulate large cell populations and cells in monolayers.

- (4) Current 3D overlapping-sphere models have not been attempted to represent epithelial cells, nor have they included polarity, nor rotational moments. Cell shape is simplified into a sphere, or ellipses. Thousands of individual cells can be simulated.
- (5) In general, two-dimensional models are better with representing local rearrangements of cells (see (Munro and Odell 2002)).

MODEL

Model background

The 2D overlapping-sphere models of an epithelial sheet and mammary gland cross-section (Shinbrot 2006; Shinbrot and Norton 2009) cells connected together on a line, so attraction was between two adjacent neighbors and new cells produced via mitosis were logically placed between two adjacent cells. In the 3D overlapping-sphere model of aggregates (Shinbrot and Norton 2009) attraction occurred between cells that were within a specific distance from each other and new cells during mitosis were placed a short distance away from the replicating cell. We remark that this is straightforward to implement in amorphous simulations; in order to maintain cells in a monolayer, however, additional constraints are needed.

Combining the simplistic 2D ordered simulation with an amorphous 3D one to create a 3D model that simulates individual cells that remain within an epithelial sheet is a difficult task. To explain, I describe the following biological facts with their corresponding modeling *strategies*:

- (1) Epithelial cells in monolayers are relatively rigid so they must resist bending of the monolayer: *Torques must be introduced into the standard overlapping-sphere model.*
- (2) Epithelial cells are polarized; they bind laterally to cells and basally to a substrate: *Interaction between cells must be based on relative orientation of the cells, not just the distance between their centers.*
- (3) Epithelial cells can move *in-plane*, especially during early development: *Interactions between cells must be strong enough to maintain an epithelium but weak enough to allow rearrangement.*
- (4) Epithelial cells can mitose *in-plane*: *The placement of new cells must not disrupt the monolayer even in places of high curvatures.*

(5) During development, cells undergo a variety of cell shape changes: *Orientation vectors must be introduced into the standard overlapping-sphere model.*

(6) The cell-cell adhesion interface is dynamic. *Introduce a method to vary the rate of attachment cells can undergo.*

In a standard overlapping-sphere model, the distance, d , between the cell centers defines the attraction between the cells (See Figure 3). A major modification to this model is that the spherical surface is taken literally as a surface from which attractive forces can act. Mechanical forces thus act at specific points on the sphere surface during attraction, similar to detailed single-cell, Adhesion Dynamics Simulations by (Hammer and Apte 1992).

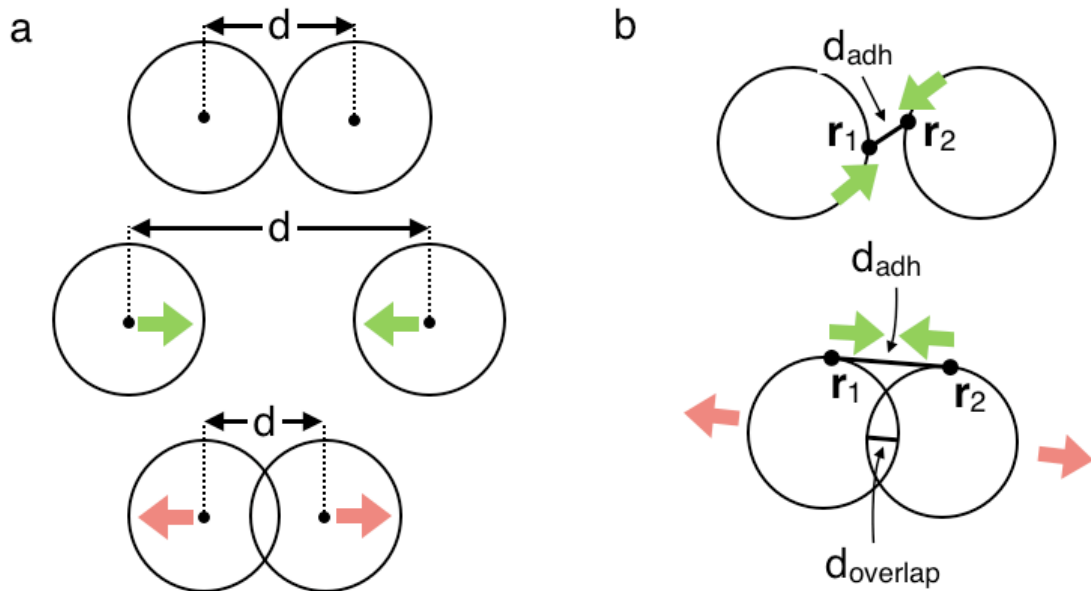


Figure 3. Comparing overlapping-sphere model with new model. (a) Attraction and repulsion forces are acted on the centers of the cells. (b) In new model, attraction forces are acting on the surface of the cell which can induce a torque, while repulsion forces act on the center of the cell.

The results of this modification include:

- (1) The opportunity to represent a cell as a surface instead of point-and-radius.
- (2) The ability to differentiate one surface of a cell from another (a crucial aspect of cell polarity).

- (3) The ability to adjust cell-interfaces in 3D space (important to simulate changes of cell shape during developmental events).
- (4) Torques that rotate cells in space (to maintain cell monolayer).

Coinciding with this new modification, is another defining feature of this model which is the adhesive link – the mechanical spring representing the source of all tensile force at our *in silico* adhesion interfaces. Details shall follow a short mathematical descriptions

Physical description of model

Our cells are modeled by spheres of mass m centered at position \mathbf{x} , where $\mathbf{x} = (x, y, z)$. They follow the master equation:

$$m \frac{d^2 \mathbf{x}}{dt^2} = \mathbf{F}_{overlap} + \mathbf{F}_{adh} + \mathbf{F}_{visc} + \mathbf{F}_{ext}$$

Where $\mathbf{F}_{overlap}$ is the net restoring force due to cell compression; \mathbf{F}_{adh} is net restoring force due to cell adhesion; \mathbf{F}_{visc} is the resistance to translation due to viscous physiological environment; and \mathbf{F}_{ext} is the external net force due to fluid or any other perturbation.

1.1 The Cell Resists Compression like a Soft Sphere

The cell model is a sphere of radius 1 and center \mathbf{x} , where $\mathbf{x} = (x, y, z)$ is a point in 3D space. All cells in our simulations occupy the same volume. To model the compressive resistance of two cells pushing against each other, we use a Hookean spring with spring coefficient $k_{overlap}$ that stretches when two spherical cell volumes overlap. The direction of this resisting force is parallel to the center-to-center vector direction, and the magnitude of this resistance follows:

$$F_{overlap} = k_{overlap} d_{overlap}, \text{ for } d < 0$$

$$F_{overlap} = 0, \text{ for } d \geq 0$$

where $d_{overlap}$ is the overlapping the distance between two cells of radius 1, with centers \mathbf{x}_i and \mathbf{x}_j ; i.e. $d_{overlap} = 2 - ||\mathbf{x}_i - \mathbf{x}_j||$. The stiffness parameter, $k_{overlap}$, represents the compressive resistance due to hydrostatic pressure and cytoskeleton stiffness. This repulsive interaction acts on the centers of the cells as depicted in Figure 4.

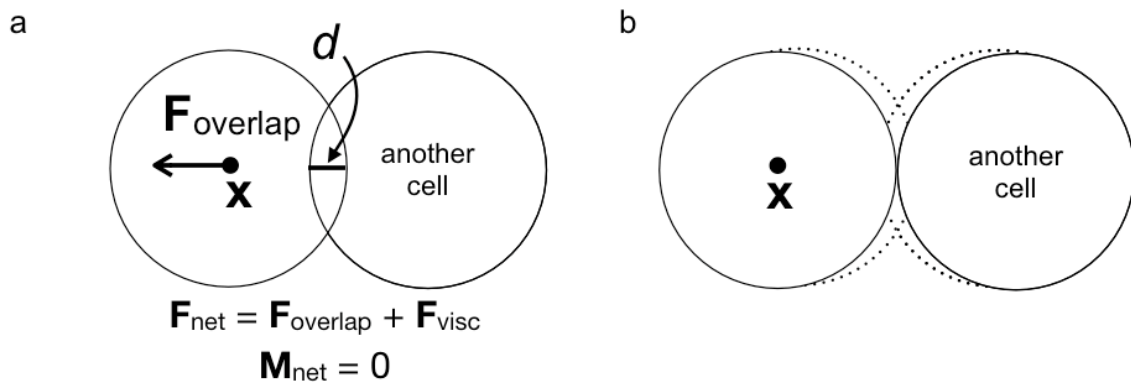


Figure 4. (a) Overlapping with another cell causes a repulsive force to push against both cells in proportion to the overlap distance, $d_{overlap}$. (Only the one overlapping force vector is shown.)

1.2 The Cell Surface Attaches to its Environment with Springs called Adhesive Links

In order for these representative cells to mechanically interact with their environment, be that another cell or a substrate, each sphere must have a mechanical component related to adhesion. The simplest component is a mechanical spring that connects the *surface* of the sphere to another sphere, to represent cell-cell adhesion, or a mechanical spring that connects the surface of a sphere model to a point in space, to represent cell-substrate adhesion.

I will refer to this spring as an *adhesive link*, because, as within the context of epithelial cells,

it is an approximation of the adhesive interface as well as the cytoskeletal filaments that attach to the underlying membrane surface of cell-cell adhesion plaques. Adhesion molecules and the cytoskeleton both resist tension in biological cells. The mere existence of an adhesive link indicates that receptor-receptor or receptor-ligand bonds have been made, and the resulting elastic properties represent the tensile properties of the cytoskeleton. In conclusion, the *adhesive link*, functions in our model as the sole element that resists stretching of biological tissue.

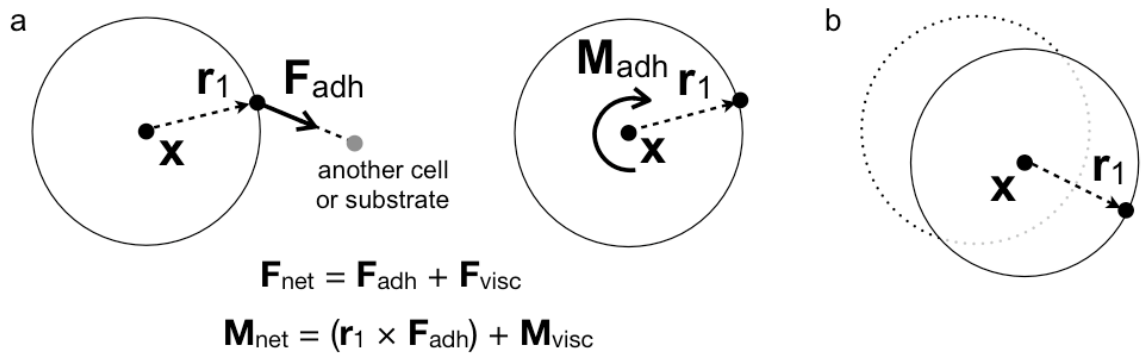


Figure 5. (a) A cell experiencing a force due to cell-cell or cell-substrate adhesion, \mathbf{F}_{adh} , at point $(\mathbf{x} + \mathbf{r}_1)$ also experiences a moment as a result of the adhesion. (b) The net force and moment translate and rotate the cell, respectively.

A cell-cell adhesive link is modeled by a spring attached to the surface of two cells, that produces the force,

$$F_{adh} = k_{adh} d_{adh}$$

The force F_{adh} acts on two points; one point on the spherical surface of cell i and the other on the spherical surface of cell j . The distance, d , is the distance between these points located at $(\mathbf{x}_i + \mathbf{r}_m)$ and $(\mathbf{x}_j + \mathbf{r}_n)$

$$d_{adh} = ||(\mathbf{x}_i + \mathbf{r}_m) - (\mathbf{x}_j + \mathbf{r}_n)||$$

The force F_{adh} is non-zero whenever neither of the attachment points are inside either cell sphere (Figure 6). This ensures that the cells' resistance to compression is dictated by the stiffness parameter $k_{overlap}$ only; that the adhesive link contributes only the tensile actions

and does not contribute to resisting compression (which is considered separately).

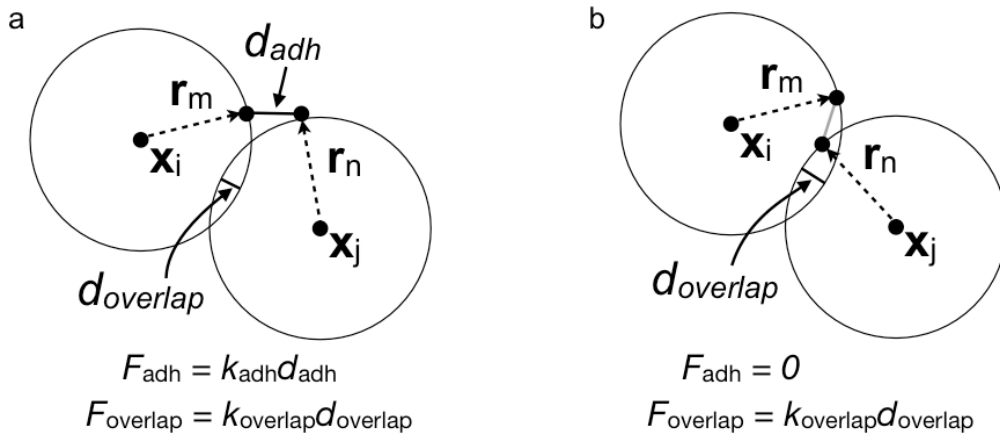


Figure 6. A pair of cells adhered to each other push and pull each other when the adhesive link is located far from the line connecting their cell centers. (b) Adhesive force is zero to ensure that compressive resistance forces are controlled by the koverlap parameter only.

The terms \mathbf{r}_m and \mathbf{r}_n are each vectors ($\mathbf{r} = [x \ y \ z]$) in \mathbb{R}^3 that define the adhesive link attachment points on each cell (Figure 6). I coin these *cytoskeleton vectors*. The adhesive stiffness parameter, k_{adh} , is a lumped parameter quantifying strength of an adhesion complex and its cytoskeleton elements enforcing it (Takeichi 1988; Hogeweg 2000; Sheth, Fontaine et al. 2000; Pokutta and Weis 2007). Each pair of cytoskeleton vectors, \mathbf{r}_m and \mathbf{r}_n , and the distance, d_{adh} , make up an *adhesive link*.

For cell-substrate adhesion, the only difference is that the adhesive link spring connects a point on the surface of a cell sphere model to an unmovable point in space. The distance, d_{adh} , would then change to $d_{adh} = \|(\mathbf{x}_i + \mathbf{r}_m) - \mathbf{y}\|$, where \mathbf{y} ($\mathbf{y} = [x \ y \ z]$) is the location of the substrate ligand in three-dimensional space.

For a cell with more than one neighbor, multiple overlap forces and adhesion forces are summed (Figure 7).

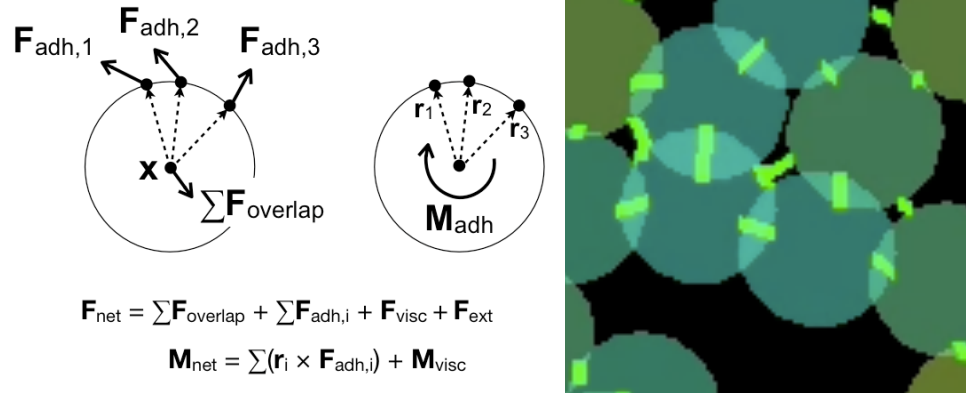


Figure 7. (a) Multiple adhesion forces, \mathbf{F}_{adh} , act simultaneously with compressive forces, $\mathbf{F}_{\text{overlap}}$. (b) A view of a sheet of cells from actual simulation shows cell spheres overlapping and connected to each other's spherical surface by adhesive links (green lines).

1.3 Force and Torque Integration

Forces are integrated using a simple forward Euler integration with a timestep of 5E-2 computational units. Since cells move in a fluid environment, a damping factor acts to reduce velocities exponentially in time, which prevents abrupt cell movements and improves computational stability (see Appendix: Viscosity for details).

After the net moment is calculated (Figure 7), the we simulated cell rotation by rotating all cytoskeleton vectors together using an angular acceleration, $\alpha = \frac{M_{\text{net}}}{I}$, where I is the dimensionless moment of inertia, and then damping the angular velocity in the same way as done for linear velocities to minimize dramatic spins, improve computational stability, and suppress inertial forces (Odell, Oster et al. 1981).

While real epithelial cells can slide past each other within a monolayer (Citi 1993), the forces in our model would restrict this in-plane movement. The torques produced by the adhesive link attractive forces would cause cells to remain ordered in their original arrangement. Therefore, I incorporated a method to reduce in-plane shear stresses, which would reduce the torque vectors pointing out of plane, and permit the sliding of epithelial

cells within the plane.

Non-slip cells assume the cell is a rigid body and that summing the torques produced by each adhesive link would rotate *all* adhesive link attachment points \mathbf{r}_i . To accomplish a slipping-interface condition, the torques from each adhesive link would rotate each adhesive link attachment point, respectively, across the surface of the cell sphere. In this condition, the adhesive link attachment points or cytoskeleton vectors are subject to the shear forces they experience at the surface of a cell sphere. I evaluated this method to see how sliding interface between cells changes the global structure.

Multiple Adhesion Molecules and Adhesive potential

In order for a cell to form an adhesive contact, it must express receptors for the appropriate type of adhesion. For example, when present in a collagen matrix, cell-cell receptors, can attach to one another, but cannot form connections with the collagen matrix. On the other hand, integrin-type receptors will bind to collagen. Our model allows each cell to individually possess a limit on the number of adhesive links it may form with cells *and* with a substrate. This is useful because it enables the testing of the differential adhesion hypothesis and direct comparisons with experimental studies that control the genetic expression of adhesion molecules.

In Aggregates, Initial Adhesion Formation is Based on Distance Thresholds

Each cell can produce an “adhesive link” with another cell once that cell is within a critical radius to the cell center. This radius has been called in previous work the *intrinsic radius* (P Pathmanathan, J Cooper et al. 2009) to contrast with the natural radius, which we simply call the radius of the sphere, that equals 1. In this work we call intrinsic radius the pseudopodal distance, d_{pseudo} , to represent the furthest distance that a cell’s arm-like

membrane processes (pseudopodia) can interact. In cell-cell adhesion formation, the adhesive link is a spring that can connect the surfaces of two spheres once the sphere surfaces are within d_{pseudo} .

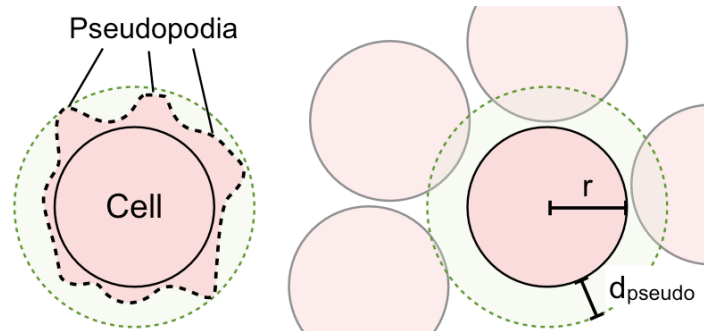


Figure 8. Like a standard overlapping-sphere model, modeling cell aggregates in 3D, we use a distance threshold before forming an adhesion. This distance, d_{pseudo} , is proportionate to the actual length of the average pseudopodia that cells actually extend during early development when probing their environment. For cells in monolayers, however, this is done differently.

In Monolayers, Initial Adhesion Formation is Based on Orientation Information Too

Another feature of the adhesive link is that its attachment can be restricted to only certain regions on the surface of the cell sphere. Given that the cell is a unit-sphere, the attachment point of the adhesive link is defined by a unit-vector – a cytoskeleton vector \mathbf{r}_i – pointing from the sphere center to the sphere surface. Therefore straightforward trigonometric computation can define where the adhesive link attaches.

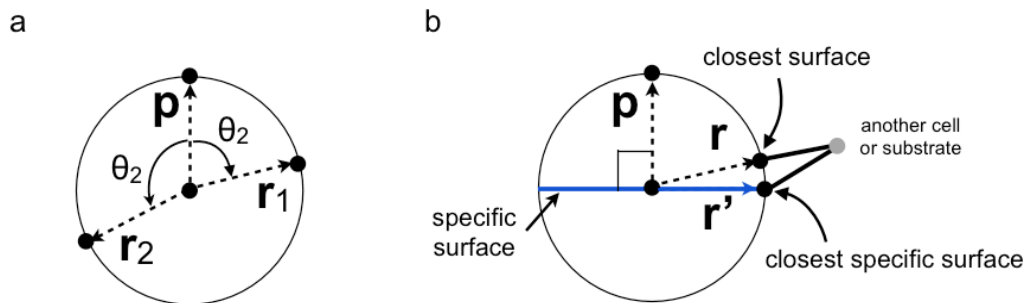


Figure 9. Specifying locations on the cell surface for a new adhesive link is possible using a point on the surface as a reference like vector, \mathbf{p} . (a) The angular distance between regions on the surface of a sphere using the cytoskeleton vector, \mathbf{r}_i , and polarity vector, \mathbf{p} , is simply the inverse cosine of the vectors' dot product. (b) I evaluated a polarity model whereby spheres may only bind to each other at a specific

This regional specificity is directly related to cell polarity, a central topic in cell research (Drubin 2000; Bryant and Mostov 2008). It is possible therefore to evaluate the function and significance of polarity within the framework of this computer model. Though we have not exhausted all parameters or geometric conditions in this topic, I have completed simulations of polarized epithelial cells that can only form adhesive links along a lateral belt so that no adhesions form near their basal or apical poles.

Two Models for a Basement Membrane

In testing ductal carcinoma models, which are epithelia in a tubular geometry, a basement membrane model is necessary for the stability of complex geometry. Although the basement membrane is actually an extracellular matrix, it is specially created by the cells at their basal poles. It is inappropriate to use the aforementioned cell-substrate model which connects the sphere surfaces to random locations in space, since it assumes an omnipresent extracellular matrix. Instead, a second of adhesion model was devised whereby a new type of adhesive link connects the basal poles of neighboring cells. The difference between this basal-basal adhesive link and the cell-cell and cell-substrate adhesive links, is that the spring already has a natural length that is double the radius of the sphere, to ensure that the poles of the spheres are not attracted to one another to the point of contact.

Since the basal connections defined in this way are attached to the cells themselves, this approach has the advantage of avoiding a separate model for a basement membrane. Nevertheless, this approach gives us the freedom to independently vary basal mechanical properties through a simple stiffness parameter. Aberrant mechanical properties of basement membranes have been implicated with cancer development after all (Zetter 1993; Butcher, Alliston et al. 2009).

Another option to modeling the basement membrane does not use any new springs, and

instead places an impenetrable, frictionless, tubular wall around the epithelium. Cells moving out of the epithelial plane would then push against this frictionless tube wall and ultimately have to move back into plane. This method for containing cells in specific geometries is common technique (Davidson, Koehl et al. 1995; Conte, Munoz et al. 2008). The advantage to this reduction in computational time, though it mainly *ensures* the geometric stability of an epithelial tube by providing an infinite resistance to mitosis.

Assumption on adhesion formation

We have not defined explicitly how molecules interact at an adhesive interface, nor do we define how long it takes before two cells are adhere to each other. We assume therefore that once an adhesion forms, i.e. a spring connects to a surface of the cell sphere model, the adhesion is fully mature. In the future it would easy to make the adhesion strength some function of time.

So far we have designated three ways of attaching two cells together.

- (1) Unpolarized cells, like cells in aggregates, form an adhesive link that connects the two closet spherical points between two spherical surfaces.
- (2) For a polarized cell, like an epithelial cell that forms lateral adhesions to its neighbors, an adhesive link connects the closest points lying on a ring that wraps around the cell (Figure 9b).
- (3) To model epithelial cells basally bound to basement membrane, a new type of adhesive link connects cells (that are already adhered to each other laterally) at between their basal poles. This basal-basal adhesive link is a spring whose natural length is twice the radius of a sphere to ensure planar geometry.

Dynamics of cell adhesion

While the biological complexity of cell adhesion is simplified by our adhesive link concept, I insist that a special feature of adhesion – that it is dynamic - must be embraced in a computer model. The adhesive-link lifetime, or link lifetime, is a parameter designed to limit the period of time that an adhesive link exerts force between two objects. Real cell interfaces are not static. They experience a lot of receptor turnover, cytoskeletal rearrangement and receptor clustering (Citi 1993; Lauffenburger and Linderman 1993; Citi 1994; Citi, Volberg et al. 1994; Sheth, Fontaine et al. 2000; Cardellini, Cirelli et al. 2007; Guillemot, Paschoud et al. 2008). Intercalation of cells is not possible without the adhesion molecules breaking old bonds and binding new ones (John Shih 1992; Brockes and Kumar 2008). Cell rearrangement phenomena are also not possible unless cells can slide past each other, which was discussed earlier with regard to integration of torques.

Our computational framework uses this lifetime parameter to control how fluid cells en masse act. The dynamics of the adhesive link can also play a role in how populations of cells maintain structure. This parameter is highlighted in the testing of cell aggregate rearrangement instead of epithelial cells because epithelial cells have more constraints with regard to adhesion formation and geometric stability. As a result, in the epithelial models, adhesive links lifetimes are infinite, they never break over time, unless of course they are stretched beyond the critical distance threshold. I foresee interesting investigation into this parameter in future work.

Modeling the Proliferation of Cells

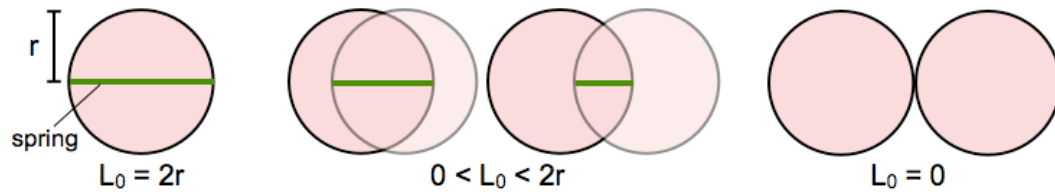


Figure 10. Mitosis is modeled by replacing the mitosing sphere by two overlapping spheres connected by an adhesive link of natural length, L_0 . Over time L_0 is reduced to 0, the default length for a cell-cell adhesive link. This ensures that new cells gradually grow into place instead of causing a new cells to suddenly be ejected out of a monolayer due to the large repulsive forces caused by overlap with new neighbors.

A cell is capable of mitosing by which a new cell is placed a small distance away. Parents and daughter cells initially overlap by a distance r to mimic the gradual enlargement of a cell during mitotic phases and not to impose sudden large repulsive forces on neighboring cells. For the same reason, new cell's repulsion spring coefficient, $k_{overlap}$ is reduced until they reach a certain age, which is arbitrarily defined.

Proliferation of cells plays a role during the model of ductal carcinoma in situ, whereby tumor cells develop at the epithelium and proliferate enough to produce finger-like projections into the tube lumen.

In addition, the mitosis model was evaluated as a function of mechanical feedback, since mitosis is the result of a complex network of events, one of which may be mechanical signaling (Canman, Hoffman et al. 2000; Brodland and Veldhuis 2002).

Modeling Cell Shape and Morphogenesis

Besides providing resistance to tensional strain, the adhesive link also *infers* the adhesive interface between two adjacent cells. Therefore, sans explicit calculation of the geometry of cell membranes, we assume that the interface between cells is the plane whose normal direction is the adhesive link direction and sits halfway along the adhesive link. To ensure that this interface is biologically accurate – especially given that actual epithelial cells often are wedge-shape in design – we define the adhesive link as a spring that connects two *cytoskeleton vectors*, each one defining the point on the surface of each adherent cell to which the adhesive link attaches. The cytoskeleton vectors effectively describe the geometric shape of an individual cell: The restoring force, due to the adhesive link stretching, causes a rotational torque within the cell, which over time equilibrates to a state where the pairs of cytoskeletal vectors spanning each adhesive link are opposite and collinear, and the adhesive link has a length of 0.

Intracellular activity is yet a well-understood aspect of cell-adhesion especially during morphogenetic events in early development (Davidson, Koehl et al. 1995; Lecuit and Lenne 2007). In this model we approach this issue carefully, with the safe assumption that the restructuring of a cell's cytoskeleton directly causes a change in cell shape. This change in cell shape would then induces some local cell rearrangement and likely some global tissue deformation.

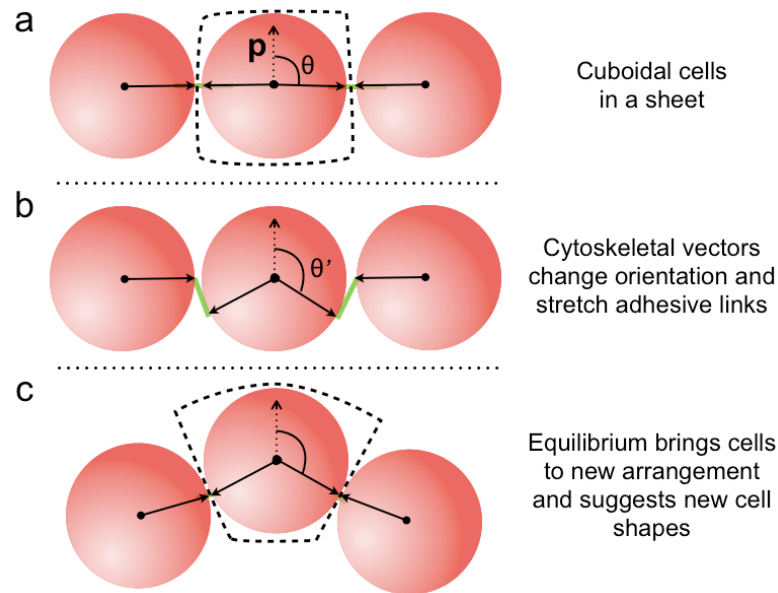


Figure 11. Cell shape change can cause tissue deformation. (a) Cells adhered to each other via a mechanical spring. (b) Reorienting a cytoskeleton vector (black arrows) of center cell relative to the cell's polarity (dotted arrow) changes spatial location of an adhesive interface, thus reshaping the cell. (c) Cells are rotated and displaces until adhesive link attachment points are touching and the cytoskeletal vectors are aligned.

The summation of the repulsive forces due to volume constraints and the attractive forces due to the alignment of cell-cell interfaces, produces a net force and a net torque that is responsible for rearranging (through translation and rotation) cells in space. Using the adhesive link as our tension-producing element and the cytoskeleton vectors as our shape and interface orientation elements, we may say how much of a role the intracellular activity (cytoskeleton vectors rotation) can affect the global intercellular interactions.

Computational Considerations

Though there is interest in the molecular events at membrane interfaces (Lauffenburger and Linderman 1993), to model this detail for several thousand cells is unfeasible and likely impractical given the amount of parameters already needed for single-cell simulations (Hammer and Apte 1992). The number of adhesion receptors on the surface of biological cells number thousands (Grasberger, Minton et al. 1986). It is for the sake of simplicity at the foundation of our computer model that we use a single mechanical spring as the basis for a cell-cell and cell-substrate adhesion. After all, even using current lab techniques it is not feasible to accurately count the number of adhesion receptors, instead a micrometer resolution is the limit for quantifying groups of receptors (Yeagle 2005). The simulation thus offers a resolution of biology comparable with that of current, popular lab technologies.

A sphere is the simplest three-dimensional volume to parameterize, as it is defined by a center point and a radius. Two-dimensional spring networks (Odell, Oster et al. 1981) require at least four points to model a cell and 3D polyhedra models require at least eight (Honda, Tanemura et al. 2004; Brodland, Chen et al. 2006) while 3D FEM models do not capture individual cells (Conte, Munoz et al. 2008) at all. The highest level of geometric detail per cell belongs to ADS models which rely on a fine mesh to model a leukocyte (~100 points).

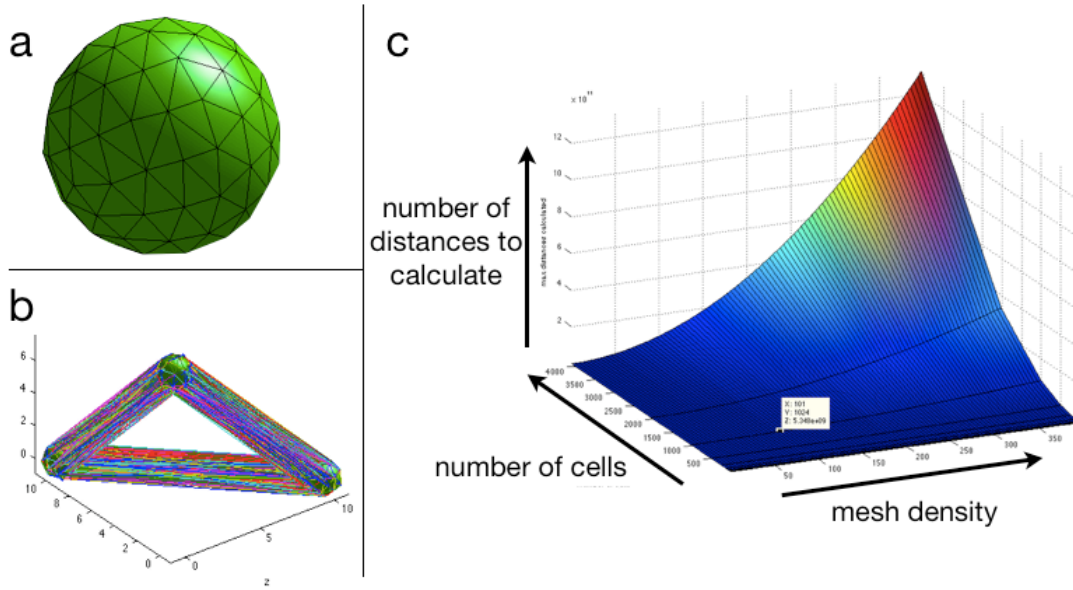


Figure 12. (a) A meshed sphere is the basic cell for a typical ADS model (Hammer and Apte 1992). It would be impractical to assume adhesion receptors exist at these mesh points and form adhesion between adjacent mesh points. Calculation time of such distances (b, drawn as colored lines) would grow exponentially (c) with the number of cells and mesh-points per cell.

Our model does not use a mesh to define receptors on a cell surface, nor does it pick points on spherical surface to calculate surface-to-surface distances (Figure 12). Instead, cells are assumed spherical and surface-to-surface distances are measured *only after* center-to-center distances are calculated, using d_{pseudo} as a threshold. There is less redundancy in calculations. Once center-to-center distances are known, we can use vectors to offset the distances if there is a specific location on the spherical surface where the adhesive link needs to attach.

Additionally, the adhesive link concept is a good compromise between the geographically-detailed ADS and the standard overlapping-sphere. The spring-elements that model small groups of adhesion molecules in ADS (Hammer and Apte 1992), 2D membrane models (Munro and Odell 2002) and Rejniak's 2D cancer model (Rejniak 2005), are grouped into an even larger representation of adhesion in our computer framework. The adhesive link

represents the mechanical properties of cell adhesion, that are provided by the adhesion molecules and the associated cytoskeleton. As, more and more research is illuminating the role of feedback and signaling in cell adhesion (Davies 2005; Chen 2008), we find the simplicity in our adhesive link model easily upgradable to a level of complexity that involves these extra dimensions of cell adhesion.

Approximately 1,000 lines of code were written in a Mathworks Matlab 2008b programming environment. See Appendix for program details.

RESULTS AND DISCUSSION

Organization of results:

- (1) Evaluate adhesion formation and adhesive potential and differential adhesion hypothesis in aggregates.
- (2) Evaluation of the basement membrane model in planar and tubular epithelia
- (3) Effects of cell shape change on global tissue structure
- (4) Effects of increasing the number of cells in tissue through mitosis
- (5) Lastly, assess the cell-substrate model for purpose of generalizing this new biological model over immotile and motile cells

Adhesion formation, adhesive potential and differential adhesion

Figure 13 demonstrates the initial adhesion formation between cells lying in the xy-plane.

The maximum surface-to-surface distance is $d_{\text{pseudo}} = r/2$, where $r = 1$. The distances between the spherical surfaces have been exaggerated so that the adhesive links (green lines) can easily be seen.

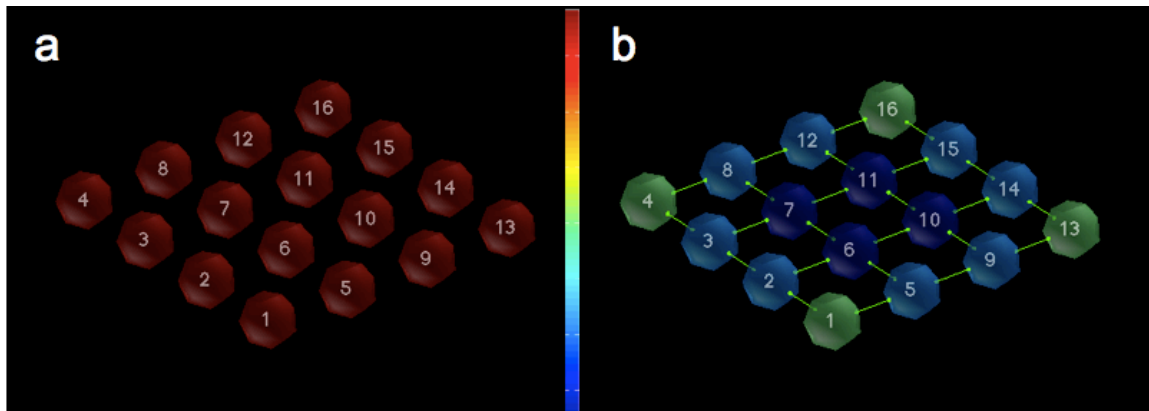


Figure 13. Cell-cell adhesion formation. (a) Sixteen cells with equal adhesive potential arranged in a regular Cartesian grid. Color of cell is proportional to adhesive potential: hot-colored cell indicates cell is capable of binding to more cells than cold colored cell. **(b)** Adhesion contact between adjacent cells represented by the *adhesive link* (green lines). Note the change in adhesive potential once a cell binds to a neighbor.

Increasing the number of adhesive links increases the probability that a cell makes adhesive contact with a nearby cell. In Figure 14, cells are prescribed their own “expression” level of a cell-cell adhesion molecule, in that they are each endowed with a different limit on the number of adhesive links each can make with their neighbors. Note that it does not require the entire population of cell to converge into a solid mass. For example, only three red cells (high adhesive potential) help to attract the 8 cells around them.

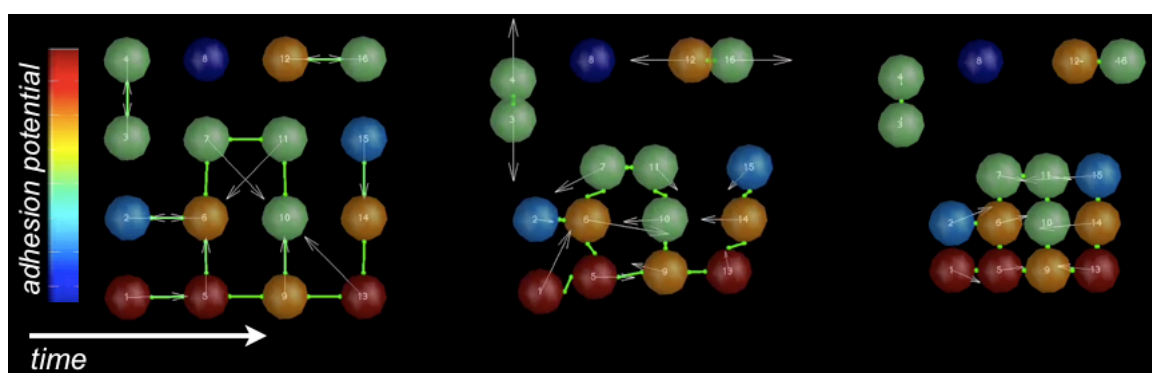


Figure 14. Cells of different adhesive potential. Sixteen cells in the xy-plane are allowed to make a maximum number of adhesive links, from 0 (dark blue) to 4 (dark red). The white arrows show the direction of the net force vector acting on each cell.

Another point is that proximity does not always guarantee that two cells will attract each other. Cells that have reached their limit of adhesive links – i.e. cell membranes that do not make available a sufficient amount of adhesion molecule – will not be able to form any adhesion. Proximity is subordinate to adhesive potential.

If the minimum adhesive potential is met and an aggregate forms out of a group of cells, as Figure 15 illustrates, an increase in adhesive potential can compact the population of cells.. It should be pointed out however, that these results are a special case of adhesion formation, in that multiple adhesive links can form between two cells. This was allowed because maintenance of a specific geometric structure is not a concern in aggregates, and multiple adhesive links between cells in monolayers may cause chaos. Fortunately, the

more chaotic the interactions in an aggregate, the more opportunity there is for cells membranes to contact, and thus form adhesive bonds.

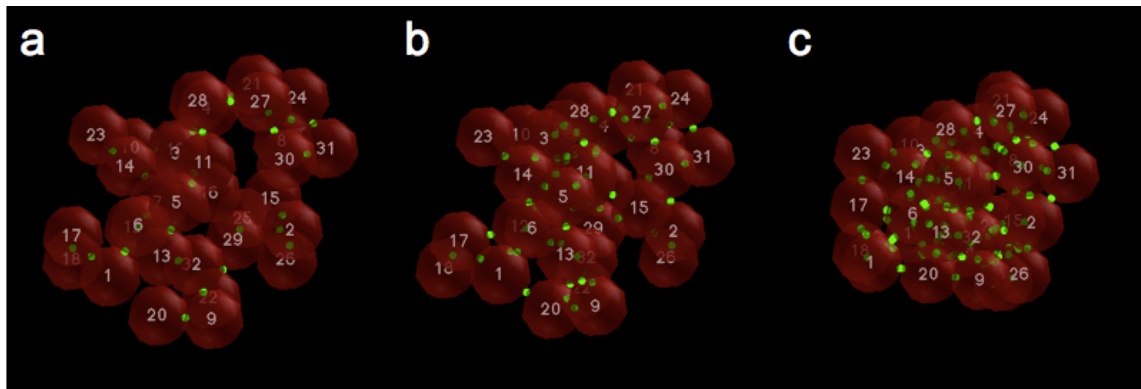


Figure 15. Adhesive potential on cell aggregates. Cells randomly clustered in space are each capable of making (a) 4, (b) 16, and (c) 64 adhesive links (green lines), effectively increasing their adhesive potential. Over time the cells (c) with the higher adhesive potential pack tighter. In this example, cells are capable of making multiple adhesive links with each of their neighbors.

Accordingly, that increasing the number of adhesive links capable of forming between cells in an aggregate tightens in the aggregate.

Since we can specify the maximum number of adhesive links each cell can make with its neighbors, we can test hypotheses based on differential adhesion (Steinberg and Poole 1981). Recall that differential adhesion hypothesis (DAH) centers around the idea that organized structures can self-assemble out of unintelligent populations of cells with distinct distributions of adhesion molecules. Figure 16 simulates the prototypical DAH experiment, whereby two groups of cells – one with a higher adhesive potential (red cells) than the other (green cells) – merge together as adhesive cells would in aggregates, until the cells with the lower adhesive potential appear to envelop the inner ones.

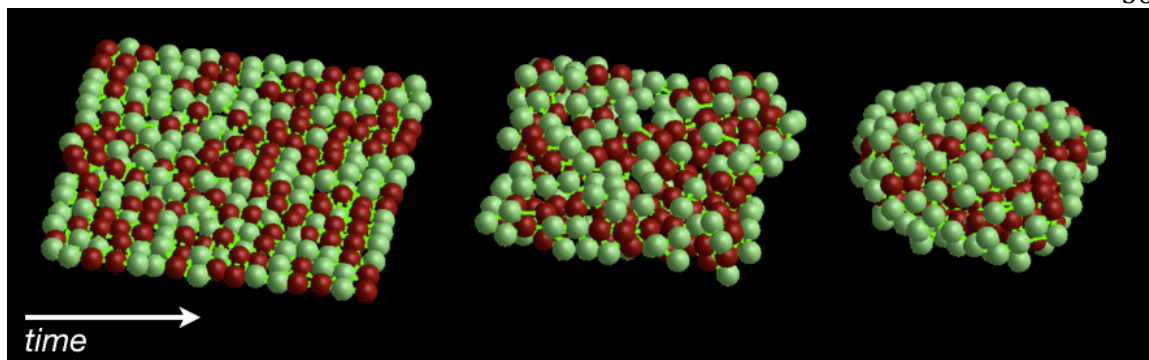


Figure 16. Red cells can make double the number of links as green cells over time this disparity in adhesive potential causes the green cells to envelope the red cells.

While some cell-sorting models depend on a parameter defining interfacial attraction, that generalizes the interface between two cells with a interfacial coefficient (Chaturvedi, Huang et al. 2005), our results uniquely attribute the organization of cell populations to a small set of parameters that are verifiable under an experimental environment. These include the adhesive spring coefficient, the number of adhesive links, and their lifetime rate. Certainly, the adhesive link is itself a lumped concept because it represents the total mechanical resistance provided by bound adhesion molecules and their associated cytoskeleton filaments. In addition, real cells have multiple contact with their environment and change their mechanical properties over time so a model parameterizing an interface by some “interfacial constant” may not be enough to make strong conclusions about the principal components of adhesion. Although the adhesive link concept is general enough to keep an overlapping-sphere model capable of simulating thousands of adhesive interfaces, it is still detailed enough to incorporate mechanical qualities like spring stiffness and dynamic parameters like the adhesive link lifetime.

Furthermore, just to contrast against adhesion models which focus on the binding of individual adhesion molecules, evidence has shown that self-organization is not due solely to the differences in adhesion molecules as DAH predicts (Shi, Chien et al. 2008). This computational model is broader in design to accommodate these new experimental insights

in self-assembly of cell aggregates in 3D.

Planar Cell Monolayers

Multicellular animals are made up of many monolayers, or sheets, of cells; they line cavities and vessels of the body. Epithelial and endothelia are the cell types that line the internal surfaces of organs and vessels so they must be able to support low and high pressure environments. We use our computational framework to model the perturbation of a single sheet of these kind of cells under different conditions.

Setting our computational model apart from typical overlapping-sphere models (P Pathmanathan, J Cooper et al. 2009) is the fact that the direction of the attraction force between cells acts on a point on the surface of a sphere instead of at the center. This allows cells to rotate their bodies and transmit a bend through the sheet. We test this ability for various conditions of a planar sheet of cells in the xy -plane where an external force, $F_z = 5$, is acting at the center of one cell and effectively pulling it out of plane.

Figure 17 compares two simulations of a perturbed planar monolayer, differing in the resistance to rotation. Softer cells, with a less developed cortical cytoskeleton would allow a folding of the sheet under constant perturbation, while rigid cells would resist tissue bending. However, in the more rigid cell monolayer, there are higher compressive forces (blue color) and more cells under very high tension (red color), which suggests that when one loses the rigidity of a cell, one is able to attenuate mechanical energy through global tissue deformation.

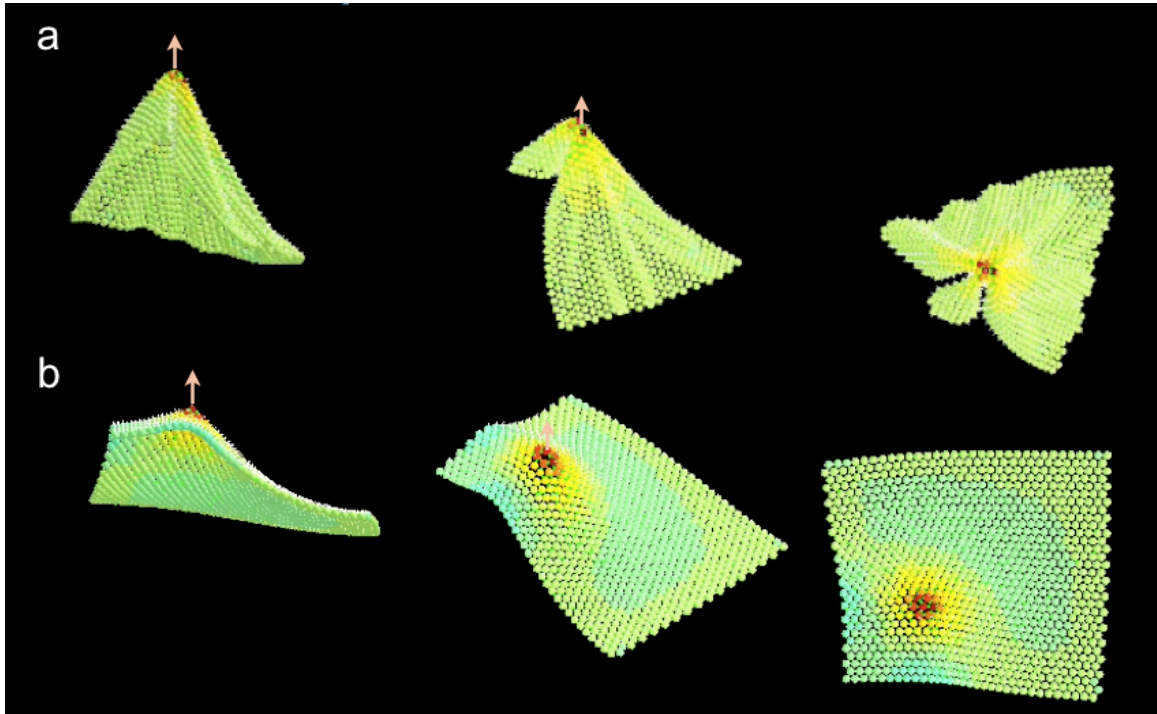


Figure 17. The perturbation of a sheet of cells for two different area moments, (a) $I_0=1$ and (b) $I_0=10$. This parameter effectively changes the rotational rigidity of the cells, or how well connected the internal cytoskeleton is. Hot colored cell experience tension while cooler colors experience compression.

Basement membrane distributes forces

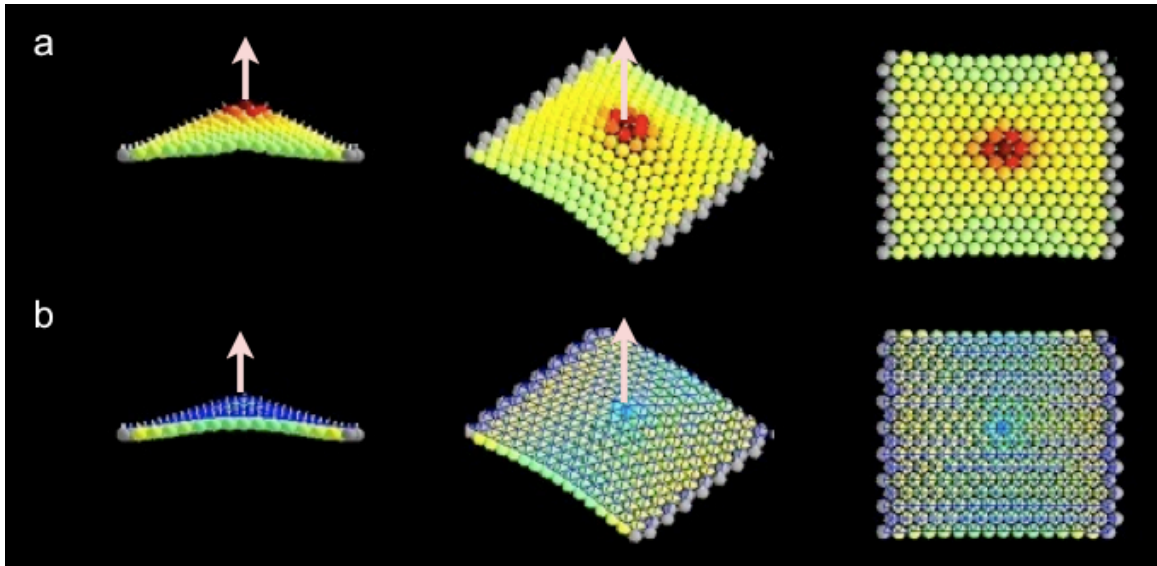


Figure 18. Basement membrane model. (a) Force perturbs a monolayer of cells, immovable at the edges (grey cells). (b) The same force perturbs a monolayer with a basement membrane and a different stress pattern appears. Hot colored cell experience tension while cooler colors experience compression.

Comparing a monolayer of cells with a *more realistic* monolayer of epithelial cells that have a basement membrane we find some convincing differences (Figure 18). First, the extremity of the tension produced at the center is completely mitigating in the basement membrane model.

The basement membrane model is open to further testing as epithelial cells experience forces from the lumen side (apical) due to fluid pressure and the basal side due to muscle contractions. Nevertheless it seems reasonable that modeling planar epithelia monolayers with a basement membrane is feasible in 3D using this overlapping-sphere model.

Slipping vs. Non-slipping Interfaces between Cells in Monolayers

Each cell-cell adhesion is represented by our adhesive link concept: a mechanical spring attached to each pair of opposing surfaces of sphere models. The displacement of the cell out of plane thus causes the stretching of its adhesive links with its three adhered neighbors, at an angle that produces a net torque for each neighbors and itself. The rotation of these three cells naturally displaces and rotates the attachment points for the adhesive links that connect to *their other* neighbors. Over time, a wave of cell-translation and – rotation travels across the cell sheet, similar to what a continuous material would do. It is the expected result that an FEM simulation is designed to reproduce (Munoz, Barret et al. 2007).

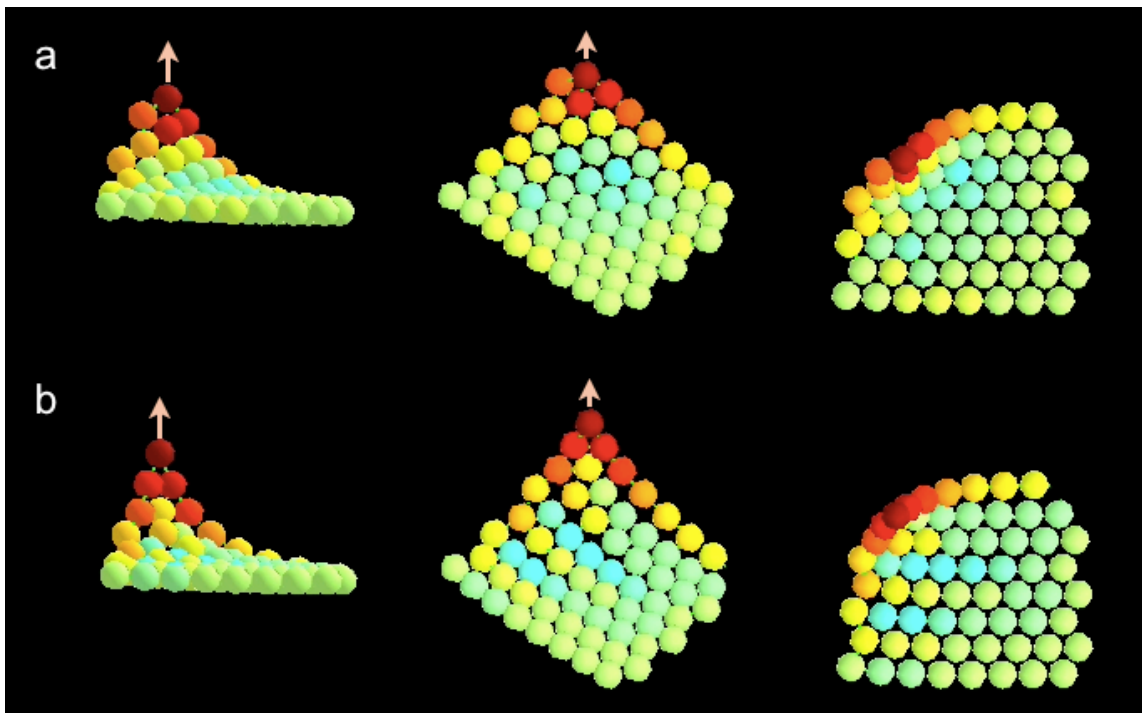


Figure 19. A hexagonally packed sheet of 64 cells existing freely in space is perturbed by a force (pink arrow), $F = 5$ in the z -direction on a corner cell. (a) Adhesive link by default are fixed to the surface of the sphere model surface and transmit torques through the cell causing an almost continuous bend through the group cells. (b) Allowing the adhesive links to slip along the surface caused sliding of layers of cells. Hotter colored cells experience tension; cold cells experience compression.

However in a biological tissue, shear forces – forces that act parallel to the surface of a cell – are not always transmitted into net torques that rotate the cells. This is therefore only appropriate if the cell has a sufficient number of adhesion molecules that are connected to a common rigid structure like a cortical cytoskeleton. For mature epithelial cells that do have a well-enforced cortical cytoskeleton (Guillemot, Paschoud et al. 2008), we see this as a good approximation.

During a period where cells are dividing and changing neighbors, this may not be appropriate model. Also if there are too few adhesion molecules and they are not very well enforced to their underlying cytoskeleton, then a shear force would break the adhesion molecule bonds, move the adhesion molecules across the membrane, or even pull the adhesion molecules out of the membrane completely. It would be convenient then if a 3D cell adhesion model could account for breaking links and moving receptor populations to a location that minimizes the shear force.

Incidentally, our model naturally accounts for adhesive breakage based on a critical force threshold as others have included in models of cell spreading (Lauffenburger and Linderman 1993). Another option we have incorporated into our model is the ability integrate the rotations of adhesive link attachment points, *separately*. So instead of contributing – that is, transmitting - the shear force to the net torque of a cell, the adhesive link alone can be pushed and pulled into a position on the cell surface that minimizes the resultant shear force. So for some adhesive links, their attachment points can displace over time according to how much shear force they each experience, while for other adhesive links, they would rotate together as one rigid body centered at the cell center. The former scenario maintains a cell-cell adhesion while simulating sliding interface associated with a highly dynamic cytoskeleton rearrangement like that identified in cell migration. The latter scenario

Figure 20b and Figure 21b illustrate the perturbation of a sheet of cells but for the case of a sliding interface. Notice how with a sliding adhesive interface, the perturbed cell loses connection with its neighbors whereas Figure 20a and Figure 21a clearly show that the perturbed cell has maintained its neighbors.

Another difference is the resulting shape of the sheet. The sliding attachment points allow the adhesive link to stretch farther in some cases causing them to break as two neighboring cells cease to be neighbors anymore. Overall, the monolayers with sliding interfaces appear flatter; they transmit less torque throughout the monolayer.

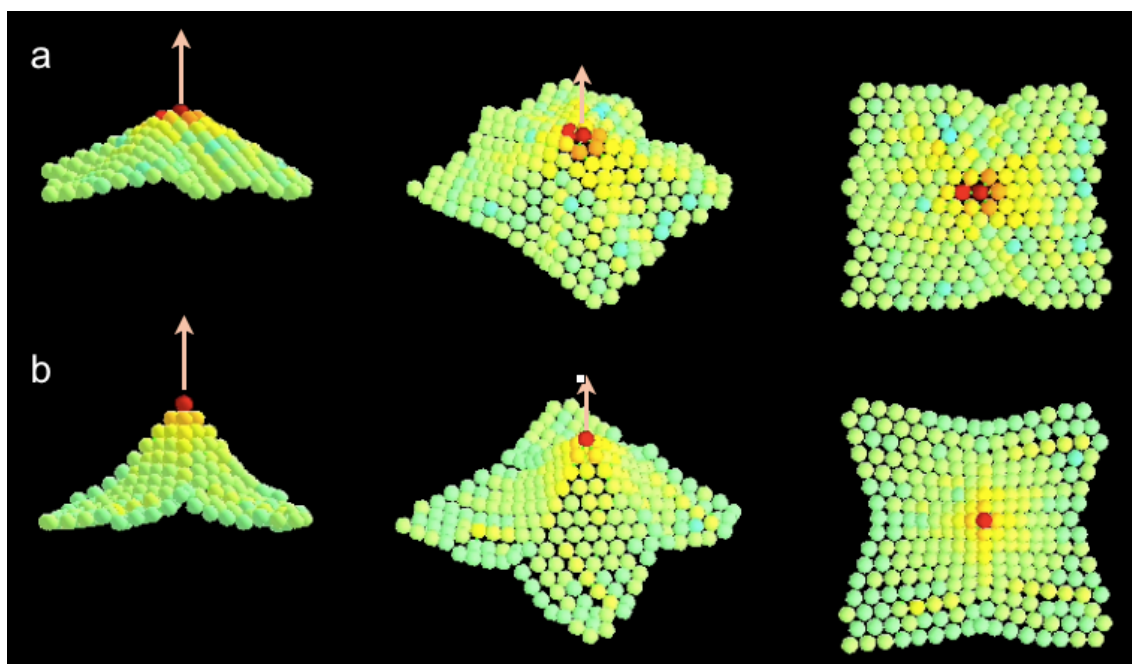


Figure 20. A hexagonally packed sheet of 256 cells existing freely in space is perturbed by a force (pink arrow), $F = 5$ in the z-direction on the centermost cell. (a) Adhesive links by default are fixed to the surface of the sphere model surface and transmit torques through the cell causing almost continuous sheet-like undulations through the group of cells. (b) Adhesive link slipping permits sliding of cells and breaking of adhesive links. Hotter colored cells experience tension; cold cells experience compression.

Epithelial cells are known to have a cortical cytoskeleton which is a network of actin

filaments underlying the cell membrane. The inner membrane domains of adhesion molecules and adhesive complexes bind to this cortical cytoskeleton for anchorage. As a result, in epithelial tissue, shear forces between cells cause a net rotation of the cells. For this reason, our model integrates forces and torques at the surface of the spheres.

However, for situations that require biological cells to be versatile, so that they actually slip past each other, intercalate with other cells (Munro and Odell 2002; Backes, Latterman et al. 2009), and perhaps undergo rearrangement due to chemical cues (Davies 2005), a less rigid interface must be considered. Within our computational framework, this means allowing the points on the surfaces of the sphere models to rotate independently of the other adhesive link attachment points.

Cells can rearrange within a sheet and within an aggregate (Citi 1994; Steinberg 2007). It is beneficial to the development of tissue that cells move past each other. Once they reach some critical period, this early tissue must be structurally stable enough so that later progenies can rearrange within and specialize into further distinct tissue. Cell-cell interfaces need to be more stable and have a solid connection with each cell's cytoskeleton, if stresses are to be resisted.

Munro and Odell have modeled a 2D membrane as a viscoelastic fluid and modeled receptor binding between adjacent membranes as springs (Munro and Odell 2002). Since binding and breaking of these receptors follow stochastic rules, the membranes move tangentially.

Cell Proliferation

Mitosis is the period during a cell's lifetime where it increases in volume and then separates into two cells. Mitosis is a complex event and requires careful coordination of several intracellular components, especially the cytoskeleton (Canman, Hoffman et al. 2000; Maddox and Burridge 2003). I have simulated the proliferation of cells in a planar and tubular geometry.

Figure 21 is a top view of cells proliferating in the xy-monolayer. Notice that the proliferation of cells in one area induces tension to the adhesive interactions around them. This gives ample hope that integrating sliding interfaces between cells in monolayers would be a promising addition to an overlapping-sphere model.

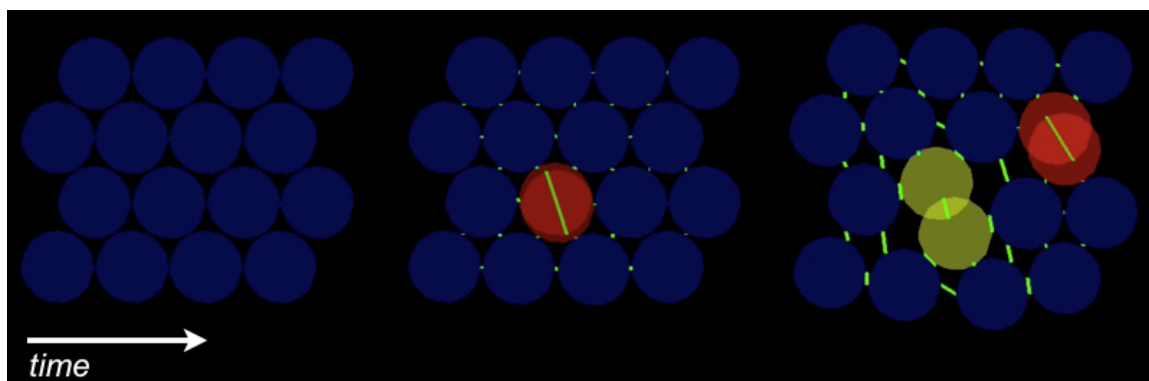


Figure 21. Mitosis in a sheet of cells. Computationally, cells separate by a spring, connecting opposite surfaces of two overlapping spheres, that reduces its natural length to zero. Colored by youth, hotter cells are younger than colder cells. (Top view)

Figure 22 takes mitosis to another level by making it a function of tension that a cell experiences, so that cells experiencing tension are . By applying a constant rightward force on the cells boxed in white, I have triggered the mitosis cycle in those cells experiencing the resulting tension, causing a spreading of the tissue in the rightward direction.

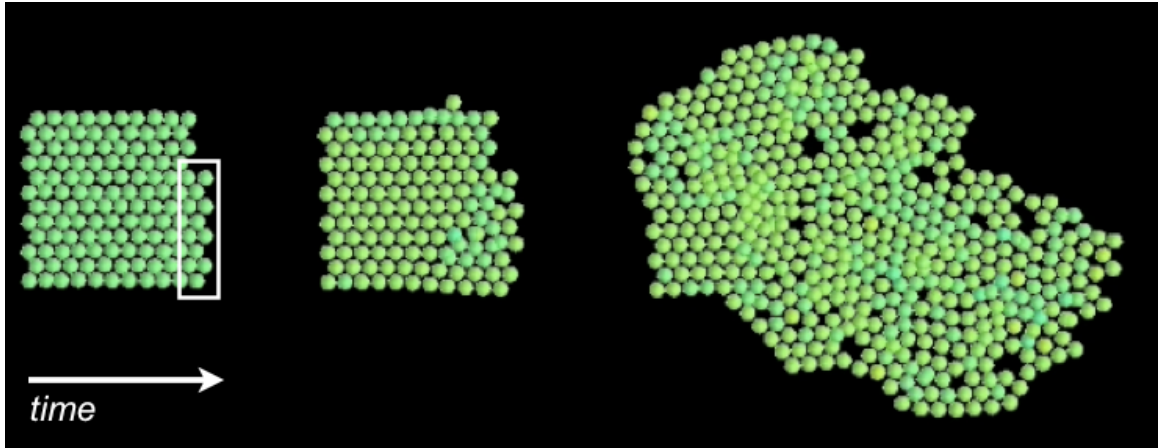


Figure 22.Feedback between tension and mitosis (top view). Cells demarcated by the white box are perturbed with a constant force to the right, while we employ a rule that states only cells under tension are allowed to mitose.

Cell Tubes and the Importance of Polarity

In an effort to understand the mechanical forces related to ductal carcinoma in situ, we find that cell-cell adhesion must be treated carefully to accommodate the complex geometry. Cells are initialized in a cylindrical arrangement, close enough to adhere to each other within the first iteration of the simulation. Tubes simulated are usually 40-50 cells in circumference which is to scale with the average mammary duct. The aspect ratio of the tubes is roughly 2:1 to catch any deformation along the length of the tube.

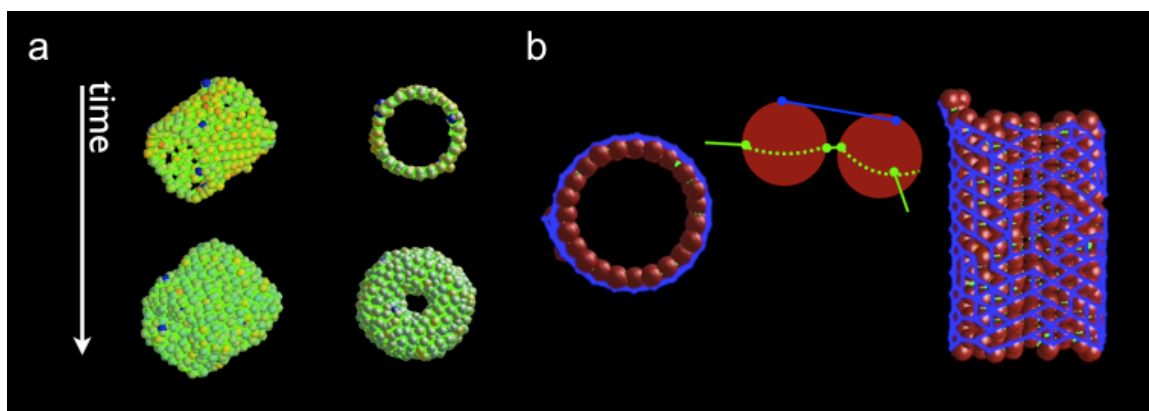


Figure 23. The demand for polarity is high especially in complex geometry. (a) Cylindrical arrangement of unpolarized cells can bond to any membrane surface and proliferation quickly causes the hollow structure to disappear. (b) Restricting cell-cell attraction to a band (dotted green line) around each cell (red sphere) to simulate a lateral adhesion in epithelia, as well as a mechanical spring (blue line) to simulate basement membrane stiffness between the basal poles of cells, we approach a more accurate picture of epithelial tubes.

Maintain the stability of a tube in three-dimensions is difficult using overlapping spheres. Under proliferating conditions, this is close to impossible. Figure 23a simulates happens when a cylindrical arrangement of non-polarized cells proliferate without basement membrane nor a polarity condition to specify the location of the adhesive links. Figure 23b conveys a tube with polarized cells *and* a basement membrane (as indicated by the blue adhesive links).

Biologically, polarity in a tubular monolayer of cells is especially important to maintain the

structure during proliferation or other mechanical perturbations. It is known for example, that polarity changes occur frequently in epithelial cells (Bryant and Mostov 2008). Cells living within a monolayer reduce their bonds with the basement membrane and migrate out of monolayer. This has great importance because there is an almost uncanny resemblance to the events that occur during tumorigenesis in mammary glands (Butcher, Alliston et al. 2009).

As these biological issues arise in a 3D world, this computational framework is designed to simulate a 3D duct. In doing so, as Figure 24 illustrates, we are able to visualize the proliferation of cells within an epithelial monolayer that is tubular in geometry.

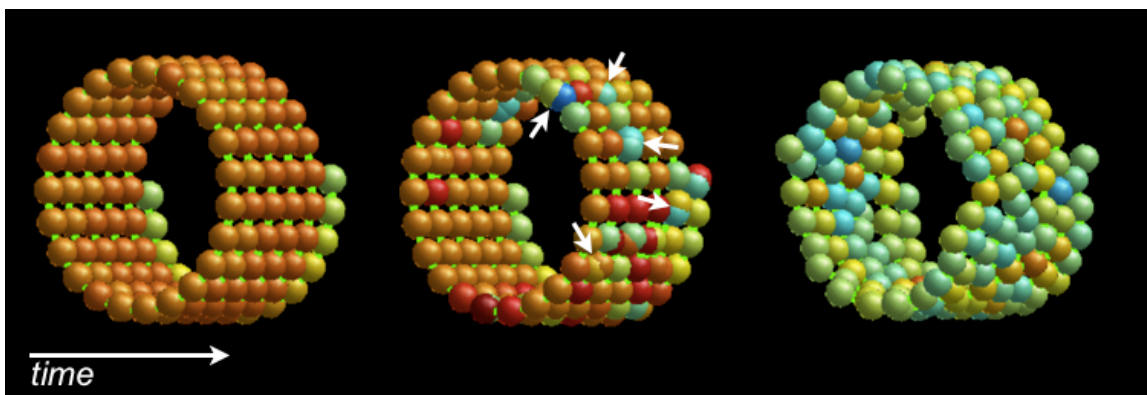


Figure 24. White arrows point to the cleavage plane of mitosing cells.

Quickly we discover however that a combination of a cell proliferation and the basement membrane that binds cell neighbors together at their basal poles, causes dramatic instabilities to the monolayer. New cells are too quickly restrained by the basement membrane model. This tells us that during mitosis in a monolayer, the formation of new cell-substrate adhesion is not instantaneous; it needs to develop with the new cell, so that the cell does not experience an environment that is “too adhesive” in which to grow. As a result, it may be possible that irregular *rates* of cell-substrate adhesion is a cause of the patterns seen in tumorous mammary gland cross-sections. Disparities between cell-

substrate and cell-cell adhesion are correlated with the tendency , though there is yet a clear consensus on what actually causes and promotes tumor development in mammary glands.

Finally the instabilities in the simulations also suggest that the current mechanical model is in need of accurate modeling of the kinetics of adhesion binding, whereby the adhesive link spring coefficient and or the adhesive potential of a cell are functions of time instead of constants. Furthermore, treatment of the cell shape may be a crucial aspect of accurate modeling of proliferation – as this is well studied in two-dimensions (Brodland and Veldhuis 2002).

Cell Shape and Morphogenesis

Apical constriction causes a narrowing of one end of an epithelial cell so that it looks more wedge-shaped and is a popular mechanism for causing developmental events seen in lens formation (Zwaan and Hendrix 1973), gastrulation (Odell, Oster et al. 1981), neuralation and drosophila appendage formation. Epithelial rearrangement hypotheses arise from the fact that epithelial cells are polarized, that they have distinct top, bottom and lateral surfaces. Each surface is characterized by the presence of specific adhesion and signaling proteins (Bryant and Mostov 2008).

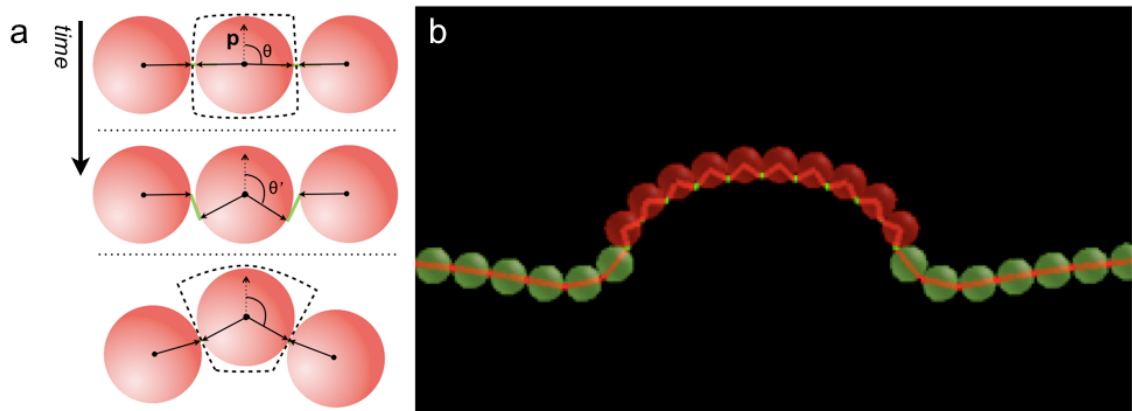


Figure 25. (a) Changing the cytoskeleton vectors (black arrows) relative to a known direction defined by polarity vector, \mathbf{p} . The adhesive link (green lines) provides the pulling force causing the overall tissue deformation see in (b) simulation (where cytoskeleton vectors are red lines).

In this model we model shape change by using a polarity vector that defines the apical-basal orientation of the cell and reorienting the cytoskeleton vectors in relation to it. For example, by changing the direction of the cytoskeleton vectors from a direction perpendicular to the polarity vector, to a direction greater or less than 90 degrees, we can produce a wedge shaped cell (Figure 25). And since the direction of a cytoskeleton vectors changes the location of the an adhesive interface with a neighboring cell, the restoring forces resulting from the adhesive interface causes a displacement of the cell.

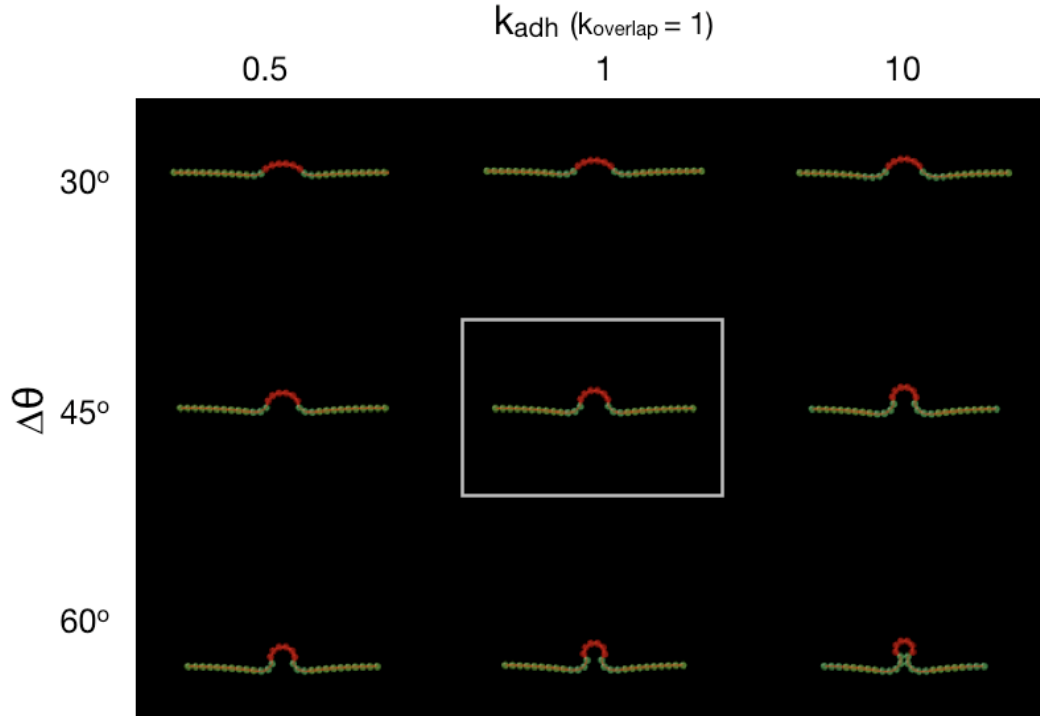


Figure 26. The effect of adhesive attraction during invagination. Six cells (red spheres) out of 32 cells become change from a cuboidal shape to a wedge-shape. The wedge acuteness is controlled by parameter $\Delta\theta$ which is the difference in angle between the current and final cytoskeletal vector directions. The boxed image is when $k_{adh} = k_{overlap} = 1$. Clearly a strong adhesion promotes invagination event.

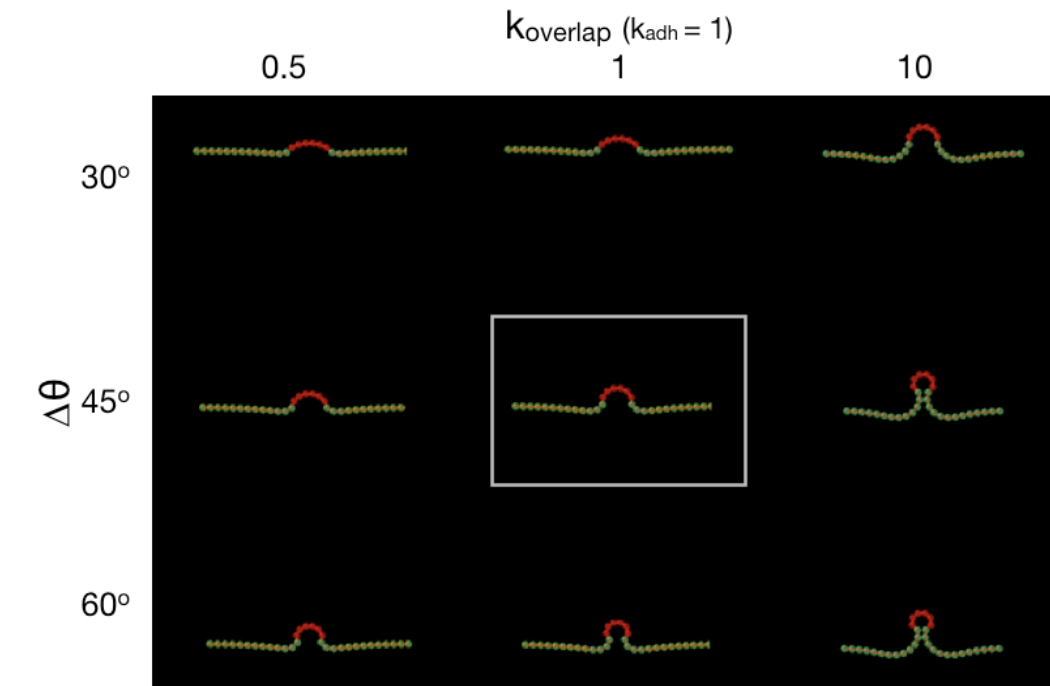


Figure 27. The effect of compressive resistance during invagination. The boxed image is when $k_{adh} = k_{overlap} = 1$. A stiffer cell appears to transmit the forces due to shape change better than a soft cell, promoting invagination.

Interestingly, increasing the compressive stiffness of a cell can have the same effect on the tissue deformation. This is possible because cell-shape change causes compression and tension on different regions of a cell – much like bending a wooden beam stretches one side and squeezes the other. A stiffer cell would more efficiently transmit the compressive forces through its body and to another cell, instead of delaying it and giving friction more opportunity to dampen it.

Our results suggests that for efficient invagination to occur, cells need to possess both a stiff cytoskeleton resistant to tension and compression. In 3D, however, this stipulation can change because the extra degrees of freedom may need to be attenuated more by a friction in order to deform the tissue stably.

Three-dimensional tissue-deformation



Figure 28. Compressive stiffness parameter, k_{overlap} , effect on an invaginating tube. During development, global structure change is accompanied by the changing of shape of a small set of cells. In comparing invagination depths, we find proper transmission of forces due this shape change requires cells to be sufficiently rigid.

Increasing the compressive stiffness has little effect on the speed of invagination in a 3D tube, however it does subtly affect the overall shape of the tube. The most stiff cells inhibit a small radius of curvature around the invagination, so the tube's curves are softer, though the depth of the invagination is larger.



Figure 29. Adhesive link stiffness parameter, k_{adh} , effect on an invaginating tube.

Increasing the resistance to tension as Figure 29 reveals is a destabilizing effect during an invagination event. While the one-dimensional invagination attempts appeared to prefer high cell stiffness and adhesion strengths, the 3D models revealed a higher sensitivity to parameters.

It is important to compare models across dimensions because the trend now is to recreate three-dimensional tissue in the lab (Griffith and Swartz 2006) as well as improve upon old methods to capture *in vivo* data (Addae-Mensah and Wikswo 2008).

Patterning of Cells Monolayers for Deformation

Regions of cells undergo cell shape change that cause global tissue deformation. We can vary the direction of the cytoskeletal vectors for specific sets of cells. The end goal of this kind of simulation is to connect the pattern that defines a group of cells in a sheet, to a architectural structure of the sheet in a sheet. A prototypical structures is a fold, which can be created by changing the shape of a cell into a wedge. With our computer model of an epithelial sheet, a wedge shape cell is produced by shrinking the angle spanning a pair opposing cytoskeleton vectors, r_i . (Actually if all opposing vectors are treated this way, the cell takes more of a cone shape.)

During the developmental event of the fly embryo monolayer of cells fold into tube-like snorkels. There are plenty of these types stories with developmental biology but few models to predict scenarios. Therefore same method used to invaginate a line and a tube was adapted to a monolayer so that the cells could mimic a cone-structure and wedges in any orientation.

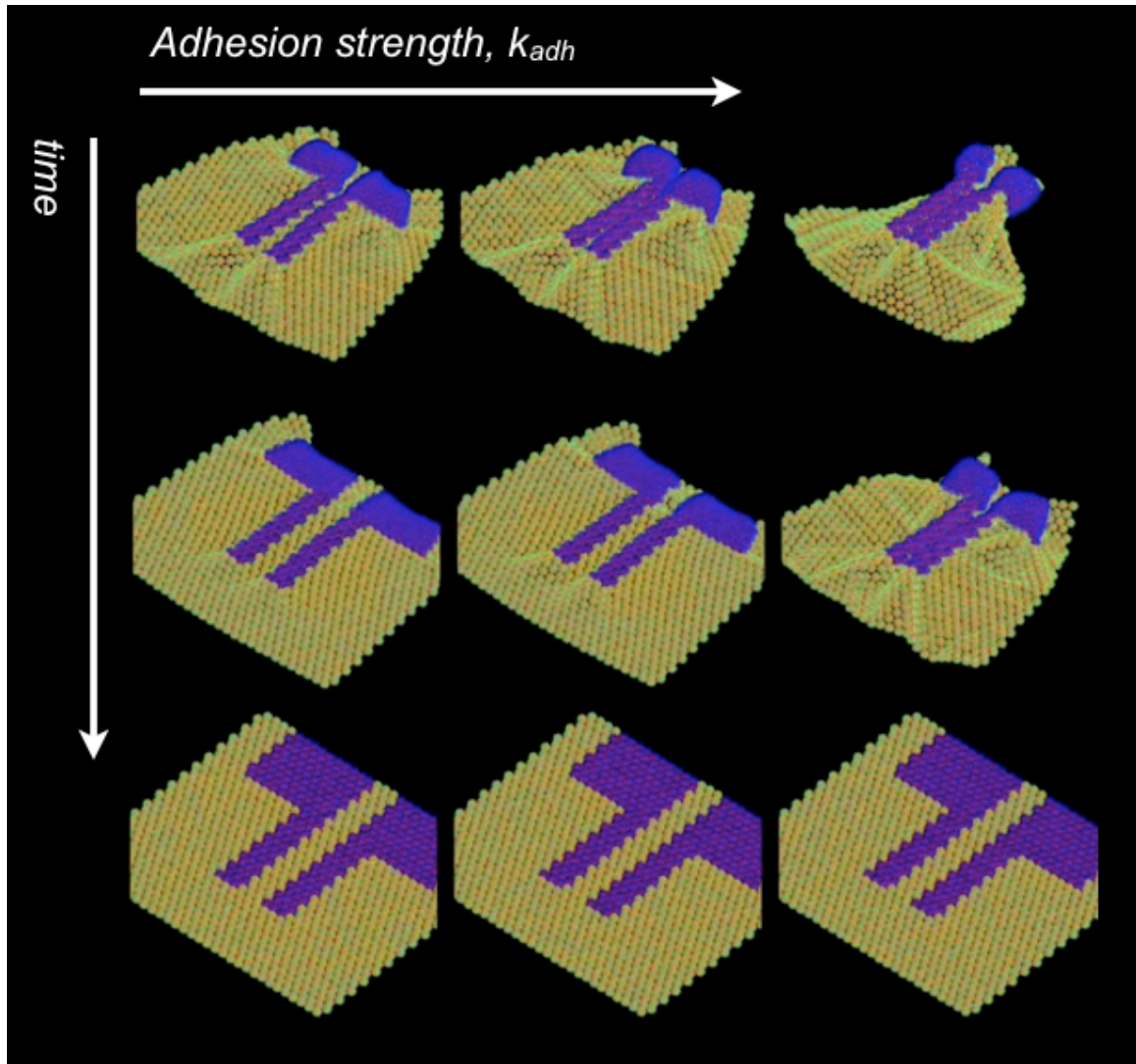


Figure 30. Patterning a sheet of cells is crucial to formation of the right kind of structure.

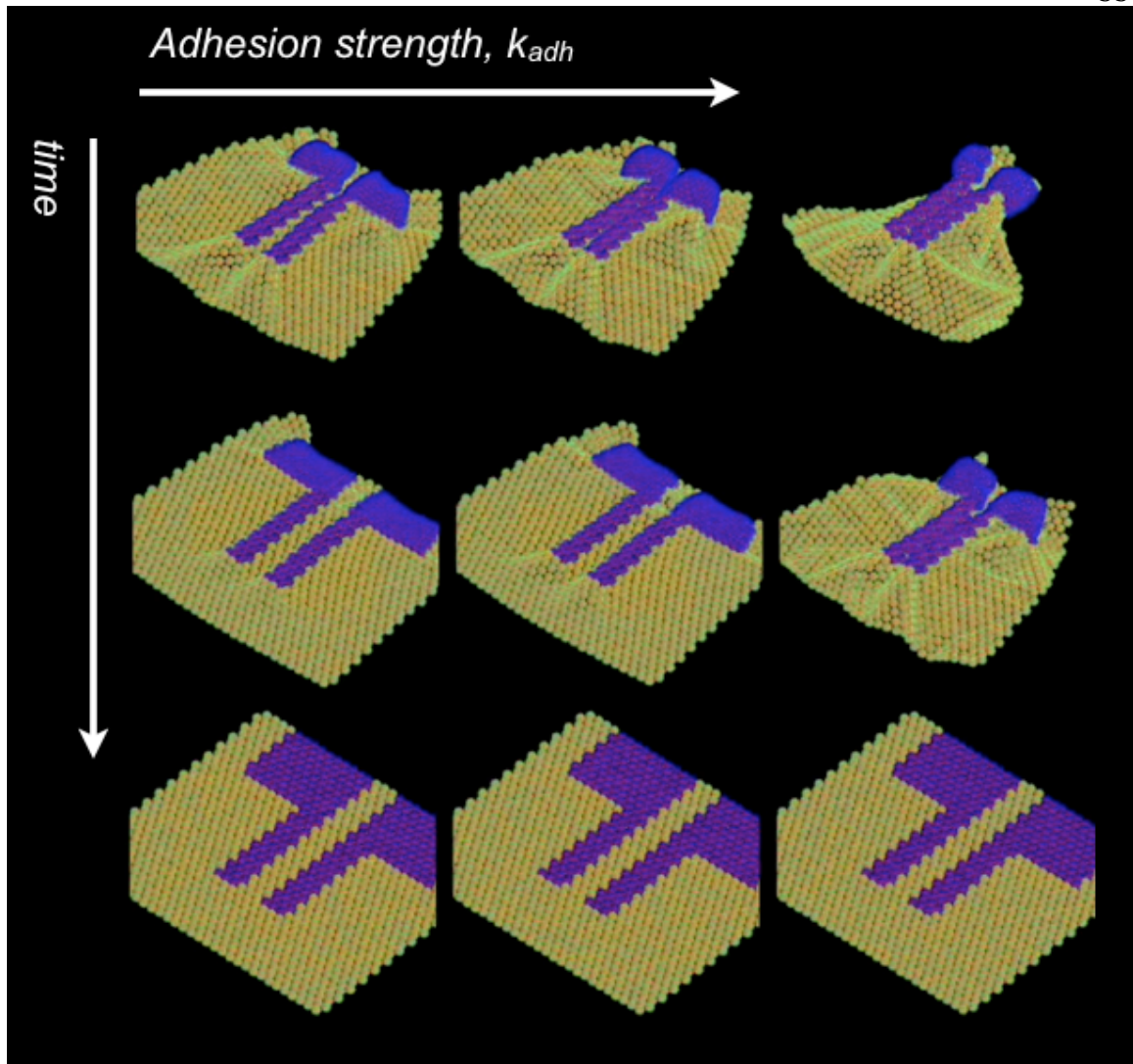


Figure 30 shows what happens when a monolayer of cells is patterned so that it causes the sheet to fold to make a tube. Though this is not the exact mechanism by which *Drosophila melanogaster* develops its “snorkel”, this does indicate that it is possible to induce interesting deformation of tissue by deforming a fraction of cells. Definitely, this is still not a complete investigation into patterning and morphogenesis as different cell-shapes, the addition of proliferating cells, and multiple patterning events are worth studying.

Exploring Cell-Substrate Interactions

The adhesive link is a mechanical spring that represents the tension producing elements of biological cells. Cell types famous for migrating and moving through cellular and extracellular tissue, like mesenchymal and fibroblastic cells, exert energy to slide actin filaments against each other in order to shift the cell's center of mass in one direction of the filament. As long as the integrin receptors on the cell membrane bind to the extracellular matrix proteins, the cell can gather enough of a footing – traction – to transmit tension throughout its body. We interpret the adhesive link as one of these tension-producing elements, so for our interpretation of cell-substrate adhesion, our model uses a special adhesive link that connects the cell

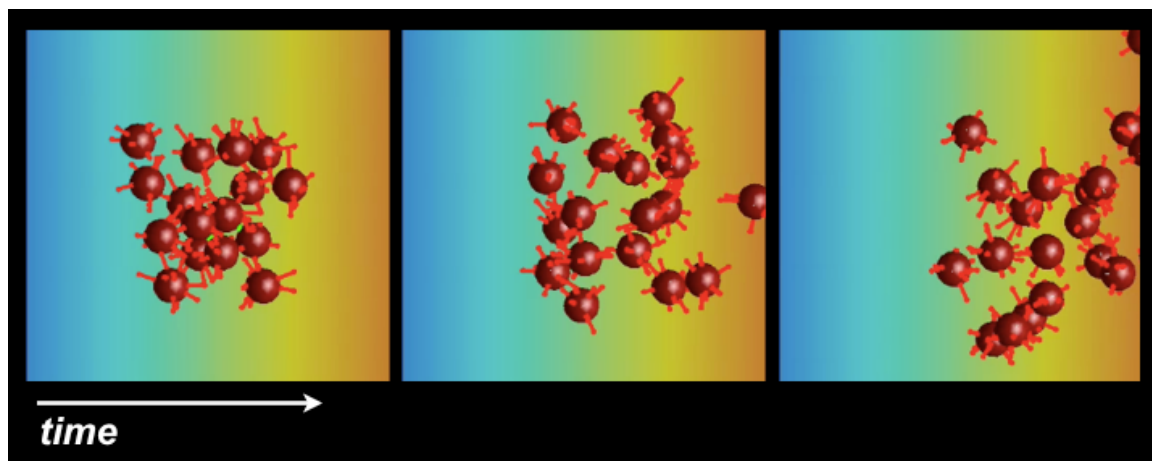


Figure 31. Migration on a stiffness gradient driven by cell-substrate adhesion. Substrate becomes stiffer as background color become hotter. Adhesive links (red lines) connect sphere surface (red spheres) to a random location in space (end of red line). Each point in space provides a spring coefficient for the adhesive link to simulate the amount of force that can be produced by the contractile machinery of that cell. Adhesive links on one side of the sphere compete with those on the opposite side.

In a *real* biological cell, the cytoskeleton would stretch the membrane to promote attachment of the available membrane receptors to an ECM fiber. In our biological model, an adhesive link is born, connected the cell sphere surface to a point in space. Where and when this occurs is currently a stochastic process in our model, and the stiffness of the

spring is defined by the substrate. A stiff substrate would call for a high k_{adh} .

As in the case for cell-cell adhesion, each cell has a limit to how many adhesive links it may form between itself and the space around it. This allows the testing of sticky cell versus non-sticky cells, to help elucidate why some cells have a stiffness preference for substrates – a counterintuitive phenomenon puzzling scientists.

Each adhesive link is a spring extending from the cell spherical surface to a point outside the cell sphere volume. This way a cell's adhesive links are always pulling against each other like a tug-of-war and the cell is the mass they are pulling. As a result, tension is *always* produced in the cell during cell-substrate adhesion. The seemingly intelligent movement of cells due to cell-substrate interactions may be due to the synergistic timing of the adhesive link formations and their placement on the cell surface.

Figure 32 shows the trajectories for 30 simulations involving a 16 cell in the middle of a stiffness gradient. Each simulation is defined by two parameters: the number of cell-substrate adhesive links acting at any one time per cell and relative steepness of the stiffness gradient. Simulation trajectories on the bottom row of boxes contain cells that have up to most mechanical springs acting on a cell at any one time, while the trajectories in the right column of boxes contain the steepest stiffness gradient. Values for the mean and standard deviation of the tortuosity of the migration trajectories are displayed in each box's top-right corner. Trajectory tortuosity is defined as the ratio between the total distance

$$\text{traveled and the displacement, } \tau = \frac{d_{travelled}}{\|\bar{x}_{final} - \bar{x}_{initial}\|}.$$

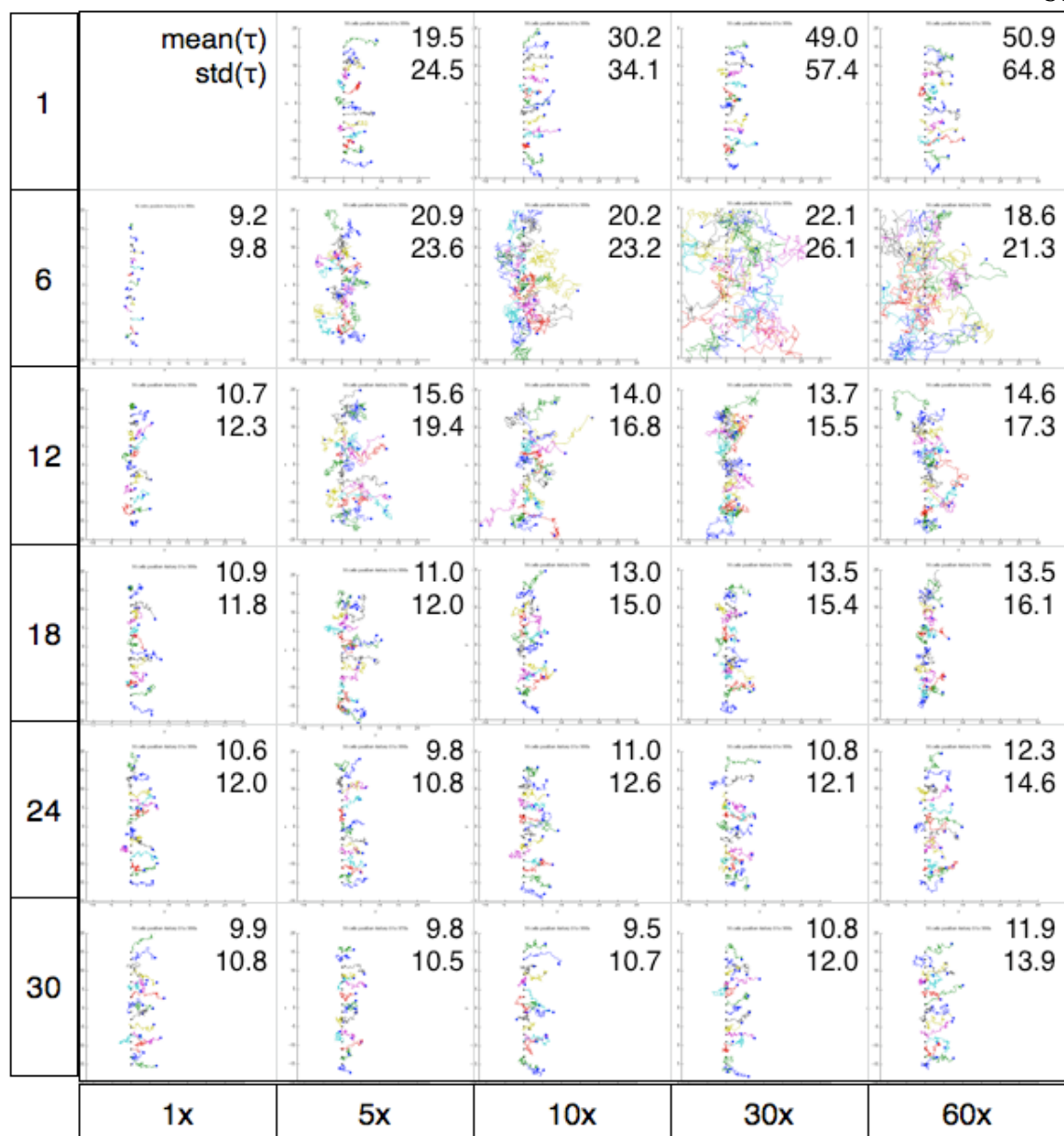


Figure 32. Thirty simulations reveal migratory trajectories are dependent on the number of adhesive links per cell (left column) and the relative steepness of the substrate stiffness gradient (bottom row). Cells on average move towards the stiffer side (right side) of substrate but through a variety of trajectories. Overlaid text shows the mean tortuosity of the trajectories and the variance of the tortuosity of the trajectories.

First, for all simulation, the variability in the tortuosity of trajectories across 16 cells was very high; the standard deviation was of the same value as the mean. As the number of adhesive links increased, the tortuosity of the trajectories decreased indicating that the cells were becoming more efficient in reaching a destination – whether they were accurately reaching a prescribed target is not being considered here, though this is the focus of other

research. This is expected because at the limit of infinite adhesive links, a cell will be pulled in the direction of the stiff gradient because the right half of sphere contains adhesive links defined by a spring coefficient larger than the adhesive links attached on the left half.

An interesting trend is that as the number of cell-substrate adhesive links increases, the total distance that the cells travel toward remains the same! the number of cells with 6 links a is the change in the trajectory morphology when one increases the number of adhesive links.

Finally, during migration, cells are known to fact polarize in the direction of their movement (Davies 2005). Their shape changes so that they lead by a wide foot trailing thin segment of their membrane. At the front, adhesion molecules are rapidly bound to the substrate and the internal cytoskeleton powers movement of the center of mass. To accommodate this kind of polarity, I would need to incorporate a regional specificity of adhesion formation similar to that applied in the epithelial cell model. This would entail creating a “zone” defined by the cell’s polarity vector and some angular range, that would be the only surface where new adhesive links may be extended into the extracellular space. Future work could make the size of this cell-substrate zone change as a function of time or as a function of tension. Future insights into polarity formation will help improve the current model for cell-substrate adhesion.

CONCLUSION

Overview:

- (1) Traditional overlapping-sphere models are based on distance-based, one-dimensional interactions to model biological cells aggregates. However this method can not model layers of cells. Our modified model adds orientation information in the form of a spherical surface to handle interactions between cells in monolayers.
- (2) In aggregates, cell populations can be sorted due to differences in the number of adhesive links – the contractile machinery distinguishing our model from other models. From our simulations, it appears that cells with a higher adhesive potential (make more adhesive links) actually *displace* the other cells because they have a higher chance of first contacting a cell neighbor and thus have a higher chance of exerting their attractive forces.
- (3) Incorporating mechanical torques, spatially specifically cell-cell contact, sliding of cell-cell contacts, and breaking of cell-cell contacts can all contribute to an accurate model of epithelial monolayers of cells.
- (4) Incorporating a basement membrane, we can also visualize the distribution of stress through a monolayer of cells, all while evaluating the effect of elastic properties which has been shown to be important in cell signaling and tumor development (Chen, Tan et al. 2004; Butcher, Alliston et al. 2009). Although FEM simulations are optimized for this kind of simulation, we can actually gather information from the individual cells experiencing the stress, and make associations between stress and other potential mechanisms like mitosis, polarity, and differentiation.
- (5) Our modified overlapping-sphere model makes it possible to simulate tubular monolayers though the extent to which the tube geometry remains stable in three-dimensions is small.
- (6) Modeling tissue deformation through cell-shape change reveals that the “hardness”

of a cell can play an equally important impact as the “stretchability”, since “harder” cells are conduits for mechanical energy to pass on through to neighboring cells.

- (7) Tissue deformation during development is often coupled with growth which was not tested, but can be.
- (8) Tension-dependent mitosis causes flatter sheets to develop than random mitosis.
- (9) Cell-substrate interaction can be modeled in this new computational framework, though further analysis into the rates of cytoskeleton extension and contraction would need to be investigated for predictions to be made.
- (10) The largest assumption, and thus the weakest aspect, of this computational framework is that cells have cube-like or spherical volumes. In reality, some types of epithelial are longer along the apico-basal axis than they are laterally, up to 5 times longer. This disparity has adversely affects the proper modeling of morphogenetic events where cell-shape change is integral to the deformation of tissue into specialized structures. I see this as the weakest aspect of the model, and would recommend simulating only cell types with small aspect ratios to reduce this disparity.

Advantages to cytoskeleton vectors

There are several advantages to using a pair of vectors to define an interface. First, as opposed to previous epithelial models that define interfaces as lines (Odell, Oster et al. 1981) or polygons (Davidson, Koehl et al. 1995; Conte, Munoz et al. 2008), one can simulate many more interfaces because one doesn’t need to initialize – and reposition – every vertex bounding the interface. Palsson (Palsson 2001; Palsson 2008) also did not model the interface and was able to simulate slug formation and movement of 4096 cell of *Dictostylea*. A hydrodynamic model. Second, cell-cell interface is generally planar and we believe that its normal direction is of importance because it suggests the cell shape as

well as potential migratory behavior. With a vector already defining this orientation, we do not need to calculate it from a set of vertices. In general it is very difficult to simulate three-dimensional geometry, so we find that by inferring the exact shape of the adhesive interface between cells and instead modeling its strain and orientation properties, we provide a very efficient approximation for epithelial tissue.

Feedback to Growth

Mechanical feedback could possibly stabilize tissue growth (Shraiman 2005). Could our model do the same? Given the results in our mitosis modeling, it is highly likely that there is a fine control over real epithelial tissue growth. For one, the basement membrane must be always in contact with new cells. Secondly, the new epithelial cells must always be in plane. Evidence of out-of-plane movements is based on cancer studies, where mammary epithelial cells either invade the lumen or invade a blood vessel (Butcher, Alliston et al. 2009). It is clear from simulations of tube ducts that mitosis provides destabilizing forces.

Membrane is domain for activity

Through a nanometer sized window, we see the cell membrane as a two-dimensional space in which lipids and proteins interact. A mathematical truth, two-dimensions is easier to fill up than three-dimensions, and as a result the membrane is a location where high concentrations of proteins can be reached more probably than in the cytoplasm. Many theoretical models (Grasberger, Minton et al. 1986) have used this two-dimensional constraint to their advantage in creating basic kinetic models that are important to our understanding of cell adhesion and signaling, especially in regards to pharmacology (Chesla, Li et al. 2000). That proteins and lipids are exchanging from the membrane to the cytoplasm, adds another level of complexity to the two-dimensional models.

Our computational model lends itself to this biological complexity because of its inherent simplicity at its basic unit, the cell. Besides ADS models (Krasik, Caputo et al. 2008) that simulate detailed cell membranes in three-dimensions, to our knowledge there are no computer models capable of simulating a membrane surface in three-dimensions for *thousands* of cells; the kind of number typically handled by a experimentalists in a Petri dish. Although it is difficult to simulate epithelial tissue using our current parameters and approximation of cell-cell and cell-substrate adhesion, we foresee an optimistic future for its fundamental features.

NEXT STEPS

There are several aspects of the current computational framework that have been explored which broaden the application of the model. Expanding on these areas will greatly enhance the merit of our biological model.

Polarity development

One of these aspects is polarity development. Given that we use a unit sphere as the representation for a biological cell, it is very simple to represent the polarity axis of a cell by a unit vector. Cell polarity has garnered a lot of interest with and is only recently being properly identified as the asymmetrical distribution of membrane properties and cytoskeletal fibers (Bryant and Mostov 2008). How the membrane evolves from a homogenous landscape to one that is two-sided is still not clear. The question is especially difficult considering the fact that highly polarized epithelial cells sitting in a monolayer can transform into less polarized, migratory mesenchymal cells. This transformation, known as the Epithelial-Mesenchyme Transition (EMT), also occurs in reverse as a Mesenchyme-Epithelial Transition (MET). These events have been shown to occur during the gastrulation phase of development (Gustafson and Wolpert 1999). Similarly, cancer of epithelial tissue has been known to be a result of a loss of polarity.

Fluorescent imaging techniques, such as FRAP, have revealed insights into the clustering nature of membrane bound adhesion receptors (Yeagle 2005; Hammond, Sim et al. 2009) while theoretical models on clusters, or receptor ‘clans’, predict that polarity does not necessarily have to follow complex signaling pathways (Altschuler, Angenent et al. 2008) and can simply self-inducing aggregates of membrane-bound adhesion molecules.

Chemical kinetic equations have been used to model the clustering of apical and basal

membrane molecules in one dimension (Altschuler, Angenent et al. 2008). Many reports agree that polarity is induced by cell-substrate adhesion (Drubin 2000). Epithelial cells for example become polarized when they have their integrin receptors firmly bound to a basement membrane.

As an aside project, I have modified the standard 3D overlapping-sphere model, so that it simulates polarity formation, hypothesizing that cell polarity could be induced primarily by cell-cell contact (Figure 33). In this model, the direction of apical-basal axis is derived from the direction of net force caused by physical contact with adjacent cells. So as cells attract each other their polarity vector changes.

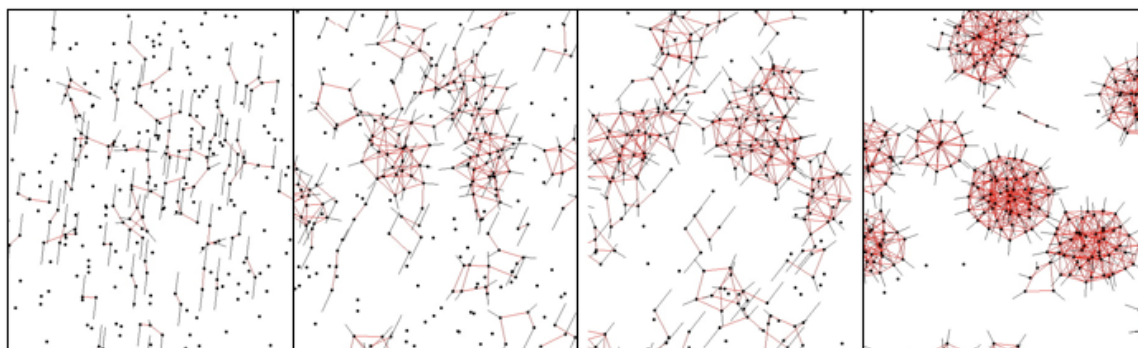


Figure 33. Standard overlapping sphere model modified with polarity formation. Cell centers (black dots) attract each other according to distance-thresholds while the orientation of each cell-cell interface (red lines) contributes to the orientation of each cell's polarity axis (black lines).

In the end however, we did not test a coupling between the *formation* of polarity and the *result* of polarity. This test model was only to assess one hypothesis in polarity formation, and not take the next step which would be to integrate feedback between the polarity axis and the spatial specificity of adhesion. It is not yet clear how the asymmetric distribution of membrane molecules causes the interactions a cell has with its environment, or vice versa. Cell polarity research has thus far been mostly descriptive and chemical in nature (Drubin 2000).

Using our computational framework, however, there is an opportunity to connect the molecular development of polarity to orientation-dependent interactions in which a cell participates. Our innovative model defines a spherical surface completely in 3D and using a few trigonometric formulas, it will be possible to simulate a molecularly heterogeneous cell membrane as (Altschuler, Angenent et al. 2008) have done in their model of polarity formation in one dimension.

Contact Area

Another important aspect to consider in future modification to the current model is the contact area of cell-cell and cell-substrate adhesion interfaces. The contact area is the planar contact between a cell and its attached surface. The initial adhering of the many adhesion molecule is cell spreading. The spreading potential of an adhesion is thus determined by the type of adhesion molecules, the inter-molecular interactions within the cell membrane and the presence of a mobile cytoskeleton behind the contact area. Researchers have used equilibrium models of cell-spreading due to receptor-ligand binding to calculate the maximal force necessary to remove a cell from a substrate (Lauffenburger and Linderman 1993).

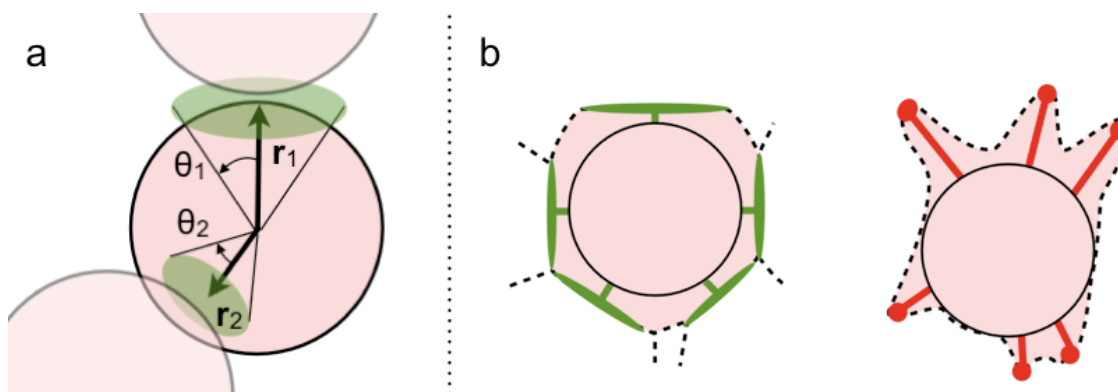


Figure 34. (a) Using vectors to represent the centers of a contact area, one can compare the direction and location of. (b) We may even be able to make distinctions between cell-cell contacts and cell-substrate contacts based on the size of the contact area and their frequency of formation.

A useful feature of using our cell sphere model is that populations of adhesion receptors can be represented by an angle, θ , that spans the diameter of a circular area sitting tangentially on the sphere, centered at an adhesive link attachment point (Figure 34). The reason for defining this area, which we term the *contact area*, is to prevent further adhesive links to attach on the sphere surface within the angular range defined by θ .

Furthermore, by increasing θ , we can dynamically simulate cell spreading (Figure 34); and start to represent the formation of an adhesion from the initial molecular binding of two cell membranes (small θ) to the micrometer-scale adhesion cluster (maximal θ). We could then distinguish mature cell adhesions from newly-formed ones. Coupled with the recent data mechanical properties of individual *molecules* (Liu, Montana et al. 2008; Thomas, Vogel et al. 2008) adding this dynamic detail to the an already three-dimensional model for a membrane may provide for some interesting, testable results.

A Flexible Biological Model

Computer simulations have been used to predict defining events in biology, suggest novel experiments and test creative theories. For example, to model epithelial tissue continua models such as finite-element models are commonly used for their accurate representation of continuous media (Davidson, Koehl et al. 1995; Conte, Munoz et al. 2008). Epithelial tissue has also been modeled by a connected network of mechanical springs (Odell (Odell, Oster et al. 1981)) while cell migration and attachment have used single cells modeled as individual fluid volumes (Hammer and Apte 1992). Complex processes that involve chemical information while losing mechanical information have been modeled by logic statements through binary decision trees (Setty, Cohen et al. 2008).

Our biological model takes a simple approach to a complex system so that it can be easily manipulated and improved with more detail as more biological truths are found. Our concept of an adhesive link is not just an individual membrane molecule, nor is it just a focal adhesion. In a cell-cell contact, the adhesive link is a unique area of contact between two adjacent cells that is the source of tensile forces between the cells; it represents the contractile machinery belonging to *both* cells. In a cell-substrate contact, the adhesive link it represents the contractile machinery of the single cell.

While some methods, even conceptually, separate the cell from its environment it is essential that attention be paid to the *relationships* between cells. This simulation adheres to the latter perspective by modeling the *connections* between cells in detail, and making assumptions on features that *do not physically interact*. Our computational model is a design of biology that corroborates the known - and the proposed - features of cells across a range of scales, environments and uncertainty. It is expected that next generation measurement devices will provide a much clearer view of the molecular components that

make up our inter-connected cellular world and the continued interplay between theory and experiment.

APPENDIX

Parameters Table

Parameter	Values tested	Description
Initial number of Cells, N	1 to 10000	Number of cells increases computation time but this time has not been calculated.
Mass of cell	1	Each cell is responds to forces in proportion to its mass. The moment of inertia, I_0 , which dictates rotational acceleration is also a function of mass.
Cell radius, r	1	Small cells have a small moment arm. Some functions that allocate initial position control the radius value so that initial positions do not cause overlap of cells. It would be better to keep the radius as a constant so that there are no scaling issues.
Spring coefficient defining cell-cell overlap repulsion	0.1 1.0	Coefficient in Hooke's law during cell-cell overlap. Approximately defines stiffness of a cell during compression.
Polarity direction	Corresponds to initial geometry	Unit-vector defining 'up-down' orientation of cell. Used as reference for defining receptor and adhesion locations relative to the cell center.
Translational viscosity	1.00 1.05 2.00 (very damped)	Frictional resistance to translational movement. Simulates a fluid environment. Prefactor of cell velocity during translational integration. ($V = V/\text{viscosity}V$) Useful to reduce oscillatory behavior.
Rotational viscosity	1.00 1.05 2.00 (very damped)	Frictional resistance to cytoskeletal movement. Simulates dampening due to a viscous fluid environment. Prefactor of angular velocity during rotational integration. ($W = W/\text{viscosity}W$) Useful to reduce oscillatory behavior.
Random velocity fluctuations	0.001 to 0.010	Adds noise to biological system. This has so far played no perceivable role and was original useful in the most simple of cell-adhesion models. It may be useful as a test for the stability of sheets and tubes
Minimum distance between two cell-equators for link to form	0.25r 0.50r	Used to simulate tight junction band around polarized epithelial cells
Minimum distance between cell surfaces needed before an adhesive may form	2r to 3r	Does not necessarily mean a bond WILL form, as is the case for equator models. This value is more of a reference to define closeness. Is there data for this value?

Maximum cytoskeletal extension (lamellopodia range)	1r	Used when simulating cytoskeletal extension into extracellular space when probing for cell-matrix attractions.
Mitosis: Rate of new cells	0.1N cell/s 0.125N cells/s 1 cell/s	Used when artificially controlling mitosis as a fixed rate. Internal control could possibly be modeled by individually triggering mitosis as a function of extracellular signals or forces, e.g. tension.
Mitosis: Critical tension	[untested]	This is a hypothesis that tension can trigger mitosis based on previous research that showed that mitosis is promoted by amount of tensions

ADHESION Parameters Table

Parameter	Values tested	Description
Types of receptor or adhesion	Cadherins (cell-cell) Integrins (cell-ECM) Basement membrane (cell-cell)	Receptor types produce adhesions independent of each other and have different properties. Multiple receptor or adhesion types can be modeled simultaneously. Basement membrane is specially treated as it is modeled by connecting the basal poles of cells with springs.
Spring coefficient defining cytoskeletal linkages per receptor type	0.1 to 10 cadherins (cell-cell) 0.1 to 1 integrins (cell-ECM) 0.1 to 10 basement membrane (cell-cell)	Coefficient in Hooke's law defines the adhesive interactions. Used as a constant coefficient, or a maximum value for a time-dependent coefficients. (3) Spring coefficient gives us a material property to the basement membrane. Could be made as a function of the lifetime of an adhesion link to simulate same-cell enhancement of adhesion junctions. This would give the simulation two forms of adhesion-enhancement, this one being the more local.
Maximum number of receptor clusters per receptor type (Equivalent to maximum number of adhesions possible per receptor type)	0 to 12 (Cell-cell: if cells are not allowed to link with the same cell twice, then value > 9 is redundant.)	Biologically defined by the level of expression of DNA. Parameter that are a function of time, tension or extracellular signals. Increasing value increases probability that adhesions will be made. Different values among cells can test differential adhesion hypothesis (Steinberg)
Age of an adhesion, AdhAge	-inf to inf s	Variable to track the development of an adhesion. Allows tracking of receptor availability and feedback loops in conjunction with MaxAdhAge parameter. Negative value (AdhAge < 0) indicates that receptors are not membrane bound and

		<p>unavailable to form an adhesion. Zero value ($\text{AdhAge} = 0$) indicates that receptors are available on the membrane, ready to form an adhesion. Positive value ($\text{AdhAge} > 0$) indicates receptor cluster is engaged in an adhesion. Existing adhesions will age dt seconds each iteration.</p> <p>Inhibited receptor clusters or receptors that are down-regulated will reduce AdhAge by subtracting large values ($>dt$) from AdhAge on down-regulating cells.</p>
Maximum age of an adhesion, MaxAdhAge	0 to inf	<p>Limits the duration that an adhesion-mediated cytoskeletal forces may act. This adds a dynamic variable to simulate the process of adhesion. Example: If value is 0, an adhesion can form apply cytoskeletal force, and break within one iteration of duration dt. Example: If value is inf adhesion will never break.</p> <p>Parameter useful for feedback loops to simulate mechanotransduction phenomena like preferential migration.</p>
Maximum distance that cytoskeletal fiber can sustain, beyond which it breaks	1r to 2r	<p>Breaking limit of adhesion. When larger than minimum membrane distance required to initially form an adhesion, this can simulate realistic stretching of adhered cells when separated.</p> <p>Is there data on how much 2 cells can strain while behind apart from each other?</p>

ENVIRONMENT

Parameter	Values tested	Description
Rate of infinite plate pushing down	0.1r units/s	Used to simulate loading tests as done in laboratories by squeezing cells between two impenetrable flat plates.
Radial force due to lumen fluid pressure	0.01 0 (none)	<p>Simulate fluid within a tube by pushing against the cells.</p> <p>Possible that this can stabilize a tube if found that a tube collapses. What are tube responses to fluid pressure?</p>
X, Y, Z limits of extracellular space	$[x, y, z] = \pm 20$	Defines the domain upon which extracellular ligand concentrations or any substrate properties can be defined.

Maximum and minimum ligand concentrations in extracellular space	Max = 1 Min = 0	Used when defining anisotropic substrate properties
Function defining the extracellular substrate properties as a function of space	$a = 1; b = 0; c = 0;$ value = $ax + by + cy$	Make 1D linear gradient if 2/3 of parameters (a,b,c) = 0. This function allows to make any sort of extracellular gradient!

GENERAL

Parameter	Values tested	Description
Time-step size	0.050 s 0.010 (current) 0.001	A comment
Simulation duration	0 to 1,000,000 s	Computation times

Derivation of viscous force

The viscous force equation in our simulation causes an exponential decay which is exactly what a fluid does. The advantage of doing this is for numerical stability. Instead of calculating $\mathbf{F}_{visc} = -\mu \frac{d\mathbf{x}}{dt}$ as done in previous simulations (Odell, Oster et al. 1981) we simply divide the cell-center velocity by a factor $\tilde{\mu}$ during Euler forward integration which ensures damping force of $\mathbf{F}_{visc} = -\left(1 - \frac{1}{\tilde{\mu}}\right) \frac{d^2\mathbf{x}}{dt^2} + \frac{1}{dt} \left(\frac{1}{\tilde{\mu}} - 1\right) \frac{d\mathbf{x}}{dt}$. Therefore equivalent damping coefficient for a dashpot in parallel is $\mu \equiv \frac{\tilde{\mu}}{dt}$ for small accelerations. This derivation is as follows:

After producing an acceleration term from intercellular interactions and using forward Euler integration, one integrates the velocity as:

$$\dot{x} \Rightarrow \dot{x} + \ddot{x}\Delta t \quad (\text{Eq. 1})$$

However to include the exponential dampening due to viscosity, this equation becomes reduced by “viscosity factor” $\tilde{\mu}$:

$$\begin{aligned} \dot{x} &\Rightarrow (\dot{x} + \ddot{x}\Delta t) \frac{1}{\tilde{\mu}} \\ \dots &\Rightarrow \frac{\dot{x}}{\tilde{\mu}} + \frac{\ddot{x}}{\tilde{\mu}} \Delta t \\ \dots &\Rightarrow \dot{x} + \left(\frac{1}{\tilde{\mu}} - 1\right) \dot{x} + \frac{\ddot{x}}{\tilde{\mu}} \Delta t \\ \dots &\Rightarrow \dot{x} + \left[\left(\frac{1}{\tilde{\mu}} - 1\right) \left(\frac{1}{\Delta t}\right) \dot{x} + \frac{\ddot{x}}{\tilde{\mu}}\right] \Delta t \\ \dots &\Rightarrow \dot{x} + \ddot{X}\Delta t \end{aligned}$$

Where \ddot{X} is the “new” acceleration, $\ddot{X} = \left(\frac{1}{\tilde{\mu}} - 1\right)\left(\frac{1}{\Delta t}\right)\dot{x} + \frac{\ddot{x}}{\tilde{\mu}}$. We then rearrange to

extract the damping component that approximates the damping coefficient of a parallel dashpot:

$$\begin{aligned}\ddot{X} &= \left(\frac{1}{\tilde{\mu}} - 1\right)\left(\frac{1}{\Delta t}\right)\dot{x} + \frac{\ddot{x}}{\tilde{\mu}} \\ \dots &= \left(\frac{1}{\tilde{\mu}} - 1\right)\left(\frac{1}{\Delta t}\right)\dot{x} + \left(\frac{1}{\tilde{\mu}} - 1\right)\ddot{x} + \ddot{x} \\ \dots &= \ddot{x} - \left[-\left(\frac{1}{\tilde{\mu}} - 1\right)\left(\frac{1}{\Delta t}\right)\dot{x} - \left(\frac{1}{\tilde{\mu}} - 1\right)\ddot{x} \right] \\ \dots &= \ddot{x} - \left[\left(1 - \frac{1}{\tilde{\mu}}\right)\left(\frac{1}{\Delta t}\right)\dot{x} + \left(1 - \frac{1}{\tilde{\mu}}\right)\ddot{x} \right]\end{aligned}$$

Where the term in square brackets is the contribution of acceleration due to damping in the general equation. For a parallel dashpot this square brackets would equate to $\mu\dot{x}$ whose dashpot coefficient is derived:

$$\begin{aligned}\mu\dot{x} &= \left(1 - \frac{1}{\tilde{\mu}}\right)\left(\frac{1}{\Delta t}\right)\dot{x} + \left(1 - \frac{1}{\tilde{\mu}}\right)\ddot{x} \\ \mu &= \left[\left(1 - \frac{1}{\tilde{\mu}}\right)\left(\frac{1}{\Delta t}\right)\dot{x} + \left(1 - \frac{1}{\tilde{\mu}}\right)\ddot{x} \right] \frac{1}{\dot{x}} \\ \mu &= \left(1 - \frac{1}{\tilde{\mu}}\right)\left(\frac{1}{\Delta t}\right) + \left(1 - \frac{1}{\tilde{\mu}}\right)\frac{\ddot{x}}{\dot{x}} \\ \mu &= \left(1 - \frac{1}{\tilde{\mu}}\right)\left(\frac{\ddot{x}}{\dot{x}} + \frac{1}{\Delta t}\right)\end{aligned}$$

As long as $\ddot{x}\Delta t \ll \dot{x}$, which occurs always for our simulations with stiffness parameters less than 10, strains less than 1, and timestep $\Delta t = 10^{-2}$:

$$\mu \cong \left(\frac{1}{\tilde{\mu}} - 1\right)\frac{1}{\Delta t} = -\frac{\tilde{\mu}}{\Delta t}$$

Using our timestep, $\Delta t = 10^{-2}$, and viscosity factor, $\tilde{\mu} = 1.05$, we achieve an equivalent dashpot damping coefficient, $\mu \cong 105$.

Algorithm Pseudo code

1. Initialization Before time-loop:.
 - a. Define Parameters (See table).
 - b. Define **adhesion** and **cells** structure variables; One adhesion structure variable per receptor type.
 - c. Cell locations in space.
2. Reduce/increase, if necessary, the ability of cells to make new links: **cell-cell links** and/or **cell-substrate**.
3. Birth new cells out of cells based on their cell features: **age** and/or **tension**.
 - a. Define properties of new cells.
4. Break adhesive links based on features: **age**, **length**, **tension**, and/or **growth**.
 - a. **Feedback**: Healthy adhesion = higher maximum age; unhealthy adhesion = lower maximum age. Healthy is related to critical adhesion tensions and maximum-age of adhesions.
 - b. Once adhesion has exceeded **maximum age**, break it.
 - c. Return the cell-cell linking- and cell-substrate linking-potential for each cell, so that cells are able to make new links.
5. Form new cell-substrate adhesions
 - a. Making of new cell-substrate links based on features: membrane extension distance, substrate existence (probabilistic or deterministic), substrate stiffness.
 - b. Find number of available cell-substrate adhesion-potential cells.
 - c. Of these potentially linkable cells, extend their surface outward to a random/exact location in space to test for substrate existence.
 - d. Define the material properties of this cell-substrate links.
 - e. Make this new cell-substrate link and record the loss of substrate linking

potential for each cell.

6. Make cell-cell adhesion (and basal-basal adhesion for basement model)
 - a. Making of new cell-cell links based on features: closeness of cells surfaces, closeness of equatorial bands of cell surfaces, and/or closeness of basal regions of cells.
 - b. Find number of available cell-cell adhesion-potential cells.
 - c. Of these potentially linkable cells, find those close to one another.
 - d. Of the cells that are close to one another, test if their surfaces are linkable which depends on the specificity on the link location, e.g. in polar cells that have an equatorial band.
 - e. Make a link between two linkable cell surfaces, and record the loss of linking potential for both cells.
7. Calculate forces of **cell-substrate**, **cell-cell**, **external body forces**, **artificial forces**, and integrate translational and rotational positions of the cells. Return to (1.)
8. Also, integrate ages of **cells** and **links**; some links may need to endure longer due to certain features like **optimal tension**.
9. Repeat 2-8 unless maximum number of iterations reached.

BIBLIOGRAPHY

- Addae-Mensah, K. A. and J. P. Wikswo (2008). "Measurement Techniques for Cellular Biomechanics In Vitro." Experimental Biology and Medicine **233**(7): 792-809.
- Altschuler, S. J., S. B. Angenent, et al. (2008). "On the spontaneous emergence of cell polarity." Nature **454**(7206): 886-889.
- Backes, T. M., R. Latterman, et al. (2009). "Convergent extension by intercalation without mediolaterally fixed cell motion." Journal of Theoretical Biology **256**(2): 180-186.
- Bell, G. I. (1978). "Models for the specific adhesion of cells to cells." Science **200**(4342): 618-627.
- Bhatia, S. K., M. R. King, et al. (2003). "The State Diagram for Cell Adhesion Mediated by Two Receptors." **84**(4): 2671-2690.
- Brookes, J. P. and A. Kumar (2008). "Comparative Aspects of Animal Regeneration." Annual Review of Cell and Developmental Biology **24**(1): 525.
- Brodland, G. W., D. I. L. Chen, et al. (2006). "A cell-based constitutive model for embryonic epithelia and other planar aggregates of biological cells." International Journal of Plasticity **22**(6): 965-995.
- Brodland, G. W. and J. H. Veldhuis (2002). "Computer simulations of mitosis and interdependencies between mitosis orientation, cell shape and epithelia reshaping." Journal of Biomechanics **35**(5): 673-681.
- Bryant, D. M. and K. E. Mostov (2008). "From cells to organs: building polarized tissue." Nat Rev Mol Cell Biol **9**(11): 887-901.
- Butcher, D. T., T. Alliston, et al. (2009). "A tense situation: forcing tumour progression." Nat Rev Cancer **9**(2): 108-22.
- Canman, J. C., D. B. Hoffman, et al. (2000). "The role of pre- and post-anaphase microtubules in the cytokinesis phase of the cell cycle." **10**(10): 611-614.
- Cardellini, P., A. Cirelli, et al. (2007). "Tight junction formation in early *Xenopus laevis* embryos: identification and ultrastructural characterization of junctional crests and junctional vesicles." Cell Tissue Res **330**(2): 247-56.
- Chaturvedi, R., C. Huang, et al. (2005). "On multiscale approaches to three-dimensional modelling of morphogenesis." Journal of The Royal Society Interface **2**(3): 237-253.
- Chen, C. S. (2008). "Mechanotransduction - a field pulling together?" J Cell Sci **121**(Pt 20): 3285-92.
- Chen, C. S., J. Tan, et al. (2004). "Mechanotransduction at Cell-Matrix and Cell-Cell Contacts." Annual Review of Biomedical Engineering **6**(1): 275-302.
- Chesla, S. E., P. Li, et al. (2000). "The Membrane Anchor Influences Ligand Binding Two-dimensional Kinetic Rates and Three-dimensional Affinity of Fcgamma RIII (CD16)." Journal of Biological Chemistry **275**(14): 10235-10246.
- Citi, S. (1993). "The molecular organization of tight junctions." J Cell Biol **121**(3): 485-9.
- Citi, S. (1994). Molecular Mechanisms of Epithelial Cell Junctions: From Development to Disease, R.G. Landes Company.
- Citi, S., T. Volberg, et al. (1994). "Cytoskeletal involvement in the modulation of cell-cell junctions by the protein kinase inhibitor H-7." J Cell Sci **107** (Pt 3): 683-92.
- Colgan, S., Ed. (2006). Cell-cell interactions : methods and protocols. Methods in molecular biology, Human Press.
- Coman, D. R. (1944). "Decreased Mutual Adhesiveness, a Property of Cells from Squamous Cell Carcinomas." Cancer Res **4**(10): 625-629.
- Conte, V., J. Munoz, et al. (2008). "A 3D finite element model of ventral furrow invagination in the *Drosophila melanogaster* embryo." Journal of the Mechanical Behavior of Biomedical Materials **1**: 188-198.
- Davidson, L. A., M. A. Koehl, et al. (1995). "How do sea urchins invaginate? Using biomechanics to distinguish between mechanisms of primary invagination." Development **121**(7): 2005-2018.
- Davies, J. A. (2005). Mechanisms of Morphogenesis, Academic Press.
- Dirk Drasdo, G. F. (2000). "Modeling the interplay of generic and genetic mechanisms in cleavage, blastulation, and gastrulation." Developmental Dynamics **219**(2): 182-191.
- Drubin, D. (2000). Cell Polarity, Oxford University Press.
- Foty, R. A. and M. S. Steinberg (2005). "The differential adhesion hypothesis: a direct evaluation." Developmental Biology **278**(1): 255-263.

- Gillespie, P. G. and R. G. Walker (2001). "Molecular basis of mechanosensory transduction." Nature **413**(6852): 194-202.
- Grasberger, B., A. P. Minton, et al. (1986). "Interaction between proteins localized in membranes." Proceedings of the National Academy of Sciences of the United States of America **83**(17): 6258-6262.
- Griffith, L. G. and M. A. Swartz (2006). "Capturing complex 3D tissue physiology in vitro." Nat Rev Mol Cell Biol **7**(3): 211-224.
- Guillemot, L., S. Paschoud, et al. (2008). "The cytoplasmic plaque of tight junctions: a scaffolding and signalling center." Biochim Biophys Acta **1778**(3): 601-13.
- Gustafson, T. and L. Wolpert (1999). "Studies on the Cellular Basis of Morphogenesis in the Sea Urchin Embryo: Directed Movements of Primary Mesenchyme Cells in Normal and Vegetalized Larvae." Experimental Cell Research **253**(2): 288-295.
- Hallstrom, W., T. Martensson, et al. (2007). "Gallium Phosphide Nanowires as a Substrate for Cultured Neurons." Nano Letters **7**(10): 2960-2965.
- Hammer, D. A. and S. M. Apte (1992). "Simulation of cell rolling and adhesion on surfaces in shear flow: general results and analysis of selectin-mediated neutrophil adhesion." **63**(1): 35-57.
- Hammond, G. R., Y. Sim, et al. (2009). "Reversible binding and rapid diffusion of proteins in complex with inositol lipids serves to coordinate free movement with spatial information." J Cell Biol **184**(2): 297-308.
- Harris, A. K., P. Wild, et al. (1980). "Silicone rubber substrata: a new wrinkle in the study of cell locomotion." Science **208**(4440): 177-179.
- Herrmann, H., H. Bar, et al. (2007). "Intermediate filaments: from cell architecture to nanomechanics." Nat Rev Mol Cell Biol **8**(7): 562-573.
- Hogeweg, P. (2000). "Evolving Mechanisms of Morphogenesis: on the Interplay between Differential Adhesion and Cell Differentiation." Journal of Theoretical Biology **203**(4): 317-333.
- Honda, H., M. Tanemura, et al. (2004). "A three-dimensional vertex dynamics cell model of space-filling polyhedra simulating cell behavior in a cell aggregate." J Theor Biol **226**(4): 439-53.
- John Shih, R. K. (1992). "Cell motility driving mediolateral intercalation in explants of *Xenopus laevis*." Development **116**: 901-914.
- Karp, G. (2008). Cell And Molecular Biology, John Wiley & Sons Inc.
- Kim, D. M. K., Andreas; Camerer, Christian; Klein, Martin (2008). "Impact of Microenvironment on the Growth of Primary Human Epidermal Cells." Journal of Craniofacial Surgery **19**(6): 1523-1525.
- King, M. R. and D. A. Hammer (2001). "Multiparticle Adhesive Dynamics. Interactions between Stably Rolling Cells." **81**(2): 799-813.
- Krasik, E. F., K. E. Caputo, et al. (2008). "Adhesive Dynamics Simulation of Neutrophil Arrest with Stochastic Activation." **95**(4): 1716-1728.
- Lauffenburger, D. A. and J. J. Linderman (1993). Receptors: Models for binding, trafficking and signaling, Oxford University Press.
- Lecuit, T. and P. F. Lenne (2007). "Cell surface mechanics and the control of cell shape, tissue patterns and morphogenesis." Nat Rev Mol Cell Biol **8**(8): 633-44.
- Liu, W., V. Montana, et al. (2008). "Comparative energy measurements in single molecule interactions." Biophys J **95**(1): 419-25.
- Lysaght, M. J. and A. L. Hazlehurst (2004). "Tissue Engineering: The End of the Beginning." Tissue Engineering **10**(1-2): 309.
- Maddox, A. S. and K. Burridge (2003). "RhoA is required for cortical retraction and rigidity during mitotic cell rounding." The Journal of Cell Biology **160**(2): 255-265.
- Martin, A. C., M. Kaschube, et al. (2009). "Pulsed contractions of an actin-myosin network drive apical constriction." Nature **457**(7228): 495-9.
- Mazzarello, P. (1999). "A unifying concept: the history of cell theory." Nat Cell Biol **1**(1): E13-E15.
- Munoz, J., K. Barret, et al. (2007). "A deformation gradient decomposition method for the analysis of the mechanics of morphogenesis." J. of Biomechanics **40**: 1372-1380.
- Munro, E. M. and G. Odell (2002). "Morphogenetic pattern formation during ascidian notochord formation is regulative and highly robust." Development **129**(1): 1-12.
- Murray, J. D. (2001). Mathematical Biology, Springer.
- Odell, G. M., G. Oster, et al. (1981). "The mechanical basis of morphogenesis. I. Epithelial folding and invagination." Dev Biol **85**(2): 446-62.
- P Pathmanathan, J Cooper, et al. (2009). "A computational study of discrete mechanical tissue

- models." Physical Biology **6**: 1-14.
- Palsson, E. (2001). "A three-dimensional model of cell movement in multicellular systems." Future Generation Computer Systems **17**: 835-852.
- Palsson, E. (2008). "A 3-D model used to explore how cell adhesion and stiffness affect cell sorting and movement in multicellular systems." Journal of Theoretical Biology **254**: 1-13.
- Pappu, V., S. K. Doddi, et al. (2008). "A computational study of leukocyte adhesion and its effect on flow pattern in microvessels." J Theor Biol **254**(2): 483-98.
- Pokutta, S. and W. I. Weis (2007). "Structure and Mechanism of Cadherins and Catenins in Cell-Cell Contacts." Annual Review of Cell and Developmental Biology **23**(1): 237-261.
- Pollack, G. H. (2001,). Cells, Gels and the Engines of Life, Ebner and Sons Publishers.
- Rejniak, K. A. (2005). "A SINGLE-CELL APPROACH IN MODELING THE DYNAMICS OF TUMOR MICROREGIONS." Mathematical Biosciences and Engineering **2**(3): 643-655.
- Roy, P., Z. Rajfur, et al. (2002). "Microscope-based techniques to study cell adhesion and migration." Nat Cell Biol **4**(4): E91-6.
- Setty, Y., I. R. Cohen, et al. (2008). "Four-dimensional realistic modeling of pancreatic organogenesis." Proceedings of the National Academy of Sciences **105**(51): 20374-20379.
- Sheetz, M. P., J. E. Sable, et al. (2006). "CONTINUOUS MEMBRANE-CYTOSKELETON ADHESION REQUIRES CONTINUOUS ACCOMMODATION TO LIPID AND CYTOSKELETON DYNAMICS." Annual Review of Biophysics and Biomolecular Structure **35**(1): 417.
- Sheth, B., J. J. Fontaine, et al. (2000). "Differentiation of the epithelial apical junctional complex during mouse preimplantation development: a role for rab13 in the early maturation of the tight junction." Mech Dev **97**(1-2): 93-104.
- Shi, Q., Y.-H. Chien, et al. (2008). "Biophysical Properties of Cadherin Bonds Do Not Predict Cell Sorting." Journal of Biological Chemistry **283**(42): 28454-28463.
- Shinbrot, T. (2006). "Simulated morphogenesis of developmental folds due to proliferative pressure." Journal of Theoretical Biology **242**(3): 764-773.
- Shinbrot, T. and K.-A. Norton (2009). "Tissue Reconstruction and Computer Model of Ductal Carcinoma in Situ." TBA.
- Shraiman, B. I. (2005). "Mechanical feedback as a possible regulator of tissue growth." Proceedings of the National Academy of Sciences of the United States of America **102**(9): 3318-3323.
- Steinberg, M. S. (2007). "Differential adhesion in morphogenesis: a modern view." Curr Opin Genet Dev **17**(4): 281-6.
- Steinberg, M. S. and T. J. Poole (1981). "Strategies for Specifying Form and Pattern: Adhesion-Guided Multicellular Assembly." Philosophical Transactions of the Royal Society of London. Series B, Biological Sciences **295**(1078): 451-460.
- Takeichi, M. (1988). "The cadherins: cell-cell adhesion molecules controlling animal morphogenesis." Development **102**(4): 639-655.
- Tepass, U., K. Truong, et al. (2000). "Cadherins in embryonic and neural morphogenesis." Nat Rev Mol Cell Biol **1**(2): 91-100.
- Thomas, W. (2008). "Catch Bonds in Adhesion." Annual Review of Biomedical Engineering **10**(1): 39-57.
- Thomas, W. E., V. Vogel, et al. (2008). "Biophysics of Catch Bonds." Annual Review of Biophysics **37**(1): 399.
- U H von Andrian, E. M. B., L Ramezani, J D Chambers, H D Ochs, J M Harlan, J C Paulson, A Etzioni, and K E Arfor (1993). "In vivo behavior of neutrophils from two patients with distinct inherited leukocyte adhesion deficiency syndromes." Journal of Clinical Investigation **91**(6): 2893-2897.
- Ward, M. D., M. Dembo, et al. (1994). "Kinetics of cell detachment: peeling of discrete receptor clusters." Biophys J **67**(6): 2522-34.
- Yamada, K. M. and K. Clark (2002). "Cell biology: survival in three dimensions." Nature **419**(6909): 790-1.
- Yeaglel, P. L., Ed. (2005). The Structure of Biological Membranes, CRC Press.
- Zetter, B. R. (1993). "Adhesion molecules in tumor metastasis." Semin Cancer Biol **4**(4): 219-29.
- Zhang, F., B. Crise, et al. (1991). "Lateral diffusion of membrane-spanning and glycosylphosphatidylinositol- linked proteins: toward establishing rules governing the lateral mobility of membrane proteins." The Journal of Cell Biology **115**(1): 75-84.
- Zwaan, J. and R. W. Hendrix (1973). "Changes in cell and organ shape during early development of the ocular lens." American Zoologist **13**: 1039-1049.